Dampened antiviral immunity to intravaginal exposure to RNA viral pathogens allows enhanced viral replication

Shahzada Khan,[1] Erik M. Woodruff,[1] Martin Trapecar,[1] Krystal A. Fontaine,[1] Ashley Ezaki,[1] Timothy C. Borbet,[1] Melanie Ott,[1,2] and Shomyseh Sanjabi[1,3]

[1]Virology and Immunology, Gladstone Institutes, San Francisco, CA 94158
[2]Department of Medicine and [3]Department of Microbiology and Immunology, University of California, San Francisco, San Francisco, CA 94143

Understanding the host immune response to vaginal exposure to RNA viruses is required to combat sexual transmission of this class of pathogens. In this study, using lymphocytic choriomeningitis virus (LCMV) and Zika virus (ZIKV) in wild-type mice, we show that these viruses replicate in the vaginal mucosa with minimal induction of antiviral interferon and inflammatory response, causing dampened innate-mediated control of viral replication and a failure to mature local antigen-presenting cells (APCs). Enhancement of innate-mediated inflammation in the vaginal mucosa rescues this phenotype and completely inhibits ZIKV replication. To gain a better understanding of how this dampened innate immune activation in the lower female reproductive tract may also affect adaptive immunity, we modeled CD8 T cell responses using vaginal LCMV infection. We show that the lack of APC maturation in the vaginal mucosa leads to a delay in CD8 T cell activation in the draining lymph node and hinders the timely appearance of effector CD8 T cells in vaginal mucosa, thus further delaying viral control in this tissue. Our study demonstrates that vaginal tissue is exceptionally vulnerable to infection by RNA viruses and provides a conceptual framework for the male to female sexual transmission observed during ZIKV infection.

INTRODUCTION

Most viral pathogens enter the host via mucosal barriers that must properly discriminate between harmful and beneficial antigens. However, when pathogens cross mucosal barriers, the host must induce an immune response (Belkaid and Naik, 2013; Perez-Lopez et al., 2016), which often involves localized inflammation and recruitment of innate immune cells that, upon arrival to the draining LN (dLN), instruct adaptive and protective immunity (Iwasaki and Medzhitov, 2015). Therefore, the early events of host response after mucosal viral infection can play a key role in determining the outcome of an infection. In particular, we know very little about the early events that result in protective immunity after vaginal infection with RNA viral pathogens.

The female reproductive tract (FRT) comprises the upper FRT (UFRT) and lower FRT (LFRT). The UFRT (endocervix, endometrium, and the fallopian tubes) is sterile and consists of type I mucosa with a monolayer of columnar epithelial cells, whereas the LFRT (vagina and ectocervix) is nonsterile, directly contacts semen antigens, and consists of type II mucosa with a multilayer of squamous epithelial cells (Iwasaki, 2010). The FRT must induce tolerance against commensals and semen antigens and also provide protection against harmful pathogens (Black et al., 2000; Moldenhauer et al., 2009; Marks et al., 2010; Ochiel et al., 2010; Kumamoto and Iwasaki, 2012; Stary et al., 2015). Although mouse models to study vaginal DNA viral infection such as HSV-1 and HSV-2 are well established, little is understood with respect to vaginal RNA virus infection because of the lack of suitable mouse models. In the face of emergent sexually transmitted RNA-viral pathogens, such as Zika virus (ZIKV) and Ebola virus (Christie et al., 2015; Musso et al., 2015; Brooks et al., 2016), and because of the absence of proper small animal models to study highly prevalent sexually transmitted retroviruses such as HIV, we lack a fundamental understanding of how the cross talk between innate and adaptive immunity occurs upon vaginal infection with this class of pathogens.

In this study, we established a mouse model of intravaginal (i.vag.) infection with a widely used model pathogen, lymphocytic choriomeningitis virus (LCMV), as well as with the Puerto Rican strain PRVABC59 (2015) of ZIKV in WT mice. LCMV is an enveloped single-stranded RNA virus of the Arenaviridae family (Zhou et al., 2012), and ZIKV is an enveloped single-stranded RNA virus of the Flaviviridae family (Lazear and Diamond, 2016). ZIKV can persist and retain infectivity in human semen long term (Harrower et al., 2016; Turmel et al., 2016), and many cases of sexual

Correspondence to Shomyseh Sanjabi: shomyseh.sanjabi@gladstone.ucsf.edu

T.C. Borbet's present address is Sackler Institute of Graduate Biomedical Sciences, New York University School of Medicine, New York, NY 10016.

Abbreviations used: CpG-ODN, CpG-oligodeoxynucleotide; dLN, draining LN; DMPA, depomedroxyprogesterone acetate; EpCam, epithelial cell adhesion molecule; FFU, focus-forming unit; FRT, female reproductive tract; iLN, iliac LN; ingLN, inguinal LN; ISG, IFN-stimulated gene; i.vag., intravaginal; LCMV, lymphocytic choriomeningitis virus; LCMV-NP, LCMV-nucleoprotein; LFRT, lower FRT; medLN, mediastinal LN; poly(I:C), polyinosinic:polycytidylic acid; qRT-PCR, quantitative RT-PCR; t.c., transcervical; UFRT, upper FRT; ZIKV, Zika virus.

The Rockefeller University Press $30.00
J. Exp. Med. 2016 Vol. 213 No. 13 2913–2929
https://doi.org/10.1084/jem.20161289

transmission have now been reported (Brooks et al., 2016; D'Ortenzio et al., 2016). Development of animal models for better understanding of ZIKV pathogenesis and for evaluating vaccine or therapeutic drug candidates is currently of utmost importance for formulating strategies to prevent and treat ZIKV infections. However, systemically and s.c. administered ZIKV cannot establish disease in WT mice because of IFN-mediated inhibition of viral replication (Grant et al., 2016; Lazear et al., 2016; Rossi et al., 2016). Unlike ZIKV, mice are the natural hosts for LCMV, and infected animals also shed virus in their feces, urine, saliva, breast milk, and semen (Barton et al., 2002). Numerous studies have used LCMV as a model system to understand the basics of antiviral immunity in mice, although vaginal infection with this virus has not been reported.

Here, we report that upon i.vag. exposure to LCMV or ZIKV, antiviral type I and III IFNs and inflammatory mediators are poorly induced in WT mouse hosts. This limited innate-mediated control of virus offers a window of opportunity for robust viral replication in the vaginal mucosa. In contrast, ZIKV fails to replicate in the LFRT tissue in the face of an ongoing systemic viral infection or when inflammation is artificially induced in the LFRT. To gain a better understanding of how this dampened innate immune activation in the LFRT may also affect adaptive immunity, we modeled CD8 T cell responses using LCMV for which T cell receptor transgenic mice are available. Limited early innate immune response during vaginal infection with LCMV also leads to significantly delayed maturation of migratory DCs (Mig DCs), causing delayed priming of CD8 T cells compared with that in i.p., transcervically (t.c.), or s.c. infected mice, thus ultimately also delaying CD8-mediated viral control in the LFRT. Our results indicate that minimal induction of antiviral IFN response in the LFRT dampens innate-mediated early control of the virus, also dampening the cross talk between innate and adaptive immunity and thus providing a loophole for robust viral replication in the vaginal mucosa. These findings have critical implications for understanding the mechanisms behind heterosexual male to female transmission of ZIKV. They also support the already observed enhanced vulnerabilities of this particular route of infection, which causes high viral titers in the vaginal mucosa of pregnant female mice, enhancing ascending infection into the fetal compartment (Yockey et al., 2016).

RESULTS

Mice are susceptible to vaginal LCMV infection

To determine whether LCMV can be vaginally infected, we i.vag. inoculated depomedroxyprogesterone acetate (DMPA; DMPA-Depo-Provera)–treated (1 mg/mouse) WT female mice with LCMV Armstrong (2×10^5 PFU), without removing the mucous layer or causing any abrasion. We found that LCMV initially infects the epithelium and then robustly replicates in the lamina propria of the LFRT in the absence of notable virus-induced damage to the vaginal tissue (Fig. 1 A). Because the i.p. route of LCMV infection generates protective immunity within the genital mucosa (Suvas et al., 2007; Casey et al., 2012; Schenkel et al., 2013), we compared the kinetics and extent of viral dissemination between DMPA-treated mice infected via i.p. (positive controls) or i.vag. routes. Using a quantitative RT-PCR (qRT-PCR) assay for LCMV (McCausland and Crotty, 2008), we detected similar levels of viral RNA per microgram of total RNA from the LFRT and iliac LN (iLN) of i.p. and i.vag. infected mice, whereas we observed very low levels of viral RNA in the spleen and other distant LNs after i.vag. infection (Fig. 1, B and C, top). Mice in their natural diestrus stage of their estrous cycle can also be infected vaginally with LCMV, although the infection rate is highly variable compared with DMPA-treated animals (Fig. 1 D). These data are the first demonstration that mice are susceptible to vaginal infection with LCMV and that LCMV can replicate in vaginal mucosa with dissemination and replication of live virus in the draining iLN.

LCMV robustly replicates in the testes after i.p. infection

We next addressed whether systemically infected male mice harbor LCMV in their testes. We detected high levels of LCMV RNA copies in testes of WT male mice 3 d after i.p. infection (Fig. 1 E). Given that high viral loads were detected in the testes of type 1 IFN receptor–deficient mice infected with ZIKV (Lazear et al., 2016), testes may represent an organ in which these RNA viruses can highly replicate in and serve as a source for sexual transmission.

LCMV robustly replicates in the LFRT with minimal induction of type I or III IFN response

To determine when and where the host detects vaginally administered LCMV, we measured the induction of IFN-β in the FRT and other peripheral tissues after infection. In i.p. infected mice, we found that IFN-β was robustly induced in the mediastinal LN (medLN), the dLN for i.p. infection (Olson et al., 2012), and in the spleen at day 1 after infection and then in various peripheral LNs at day 2 after infection (Fig. 1 B, bottom). Surprisingly, although after both i.p. and i.vag. infection viral load increased exponentially in the LFRT, viral replication resulted in very low level of IFN-α or -β mRNA induction (Fig. 1 C, bottom; and Fig. 1 F). IFN-β induction was similar in the iLNs of i.p. and i.vag. infected mice, consistent with similar kinetics and magnitude of viral replication (Fig. 1 C). However, robust IFN-β induction was not observed in the spleen of i.vag. infected animals, consistent with minimal dissemination of LCMV to the spleen (Fig. 1 C). All nucleated cells are believed to respond to IFN-α and -β, but epithelial cells respond largely to IFN-λ (type III IFN; Mahlakõiv et al., 2015). However, IFN-λ was also variably and minimally induced in the LFRT after i.p. or i.vag. infection (Fig. 1 F). Furthermore, no significant induction of IFN-α, -β, or -λ was observed in i.vag. LCMV-infected animals that were infected during their natural diestrus stage of estrous cycle (Fig. 1 G), demonstrating that the dampened

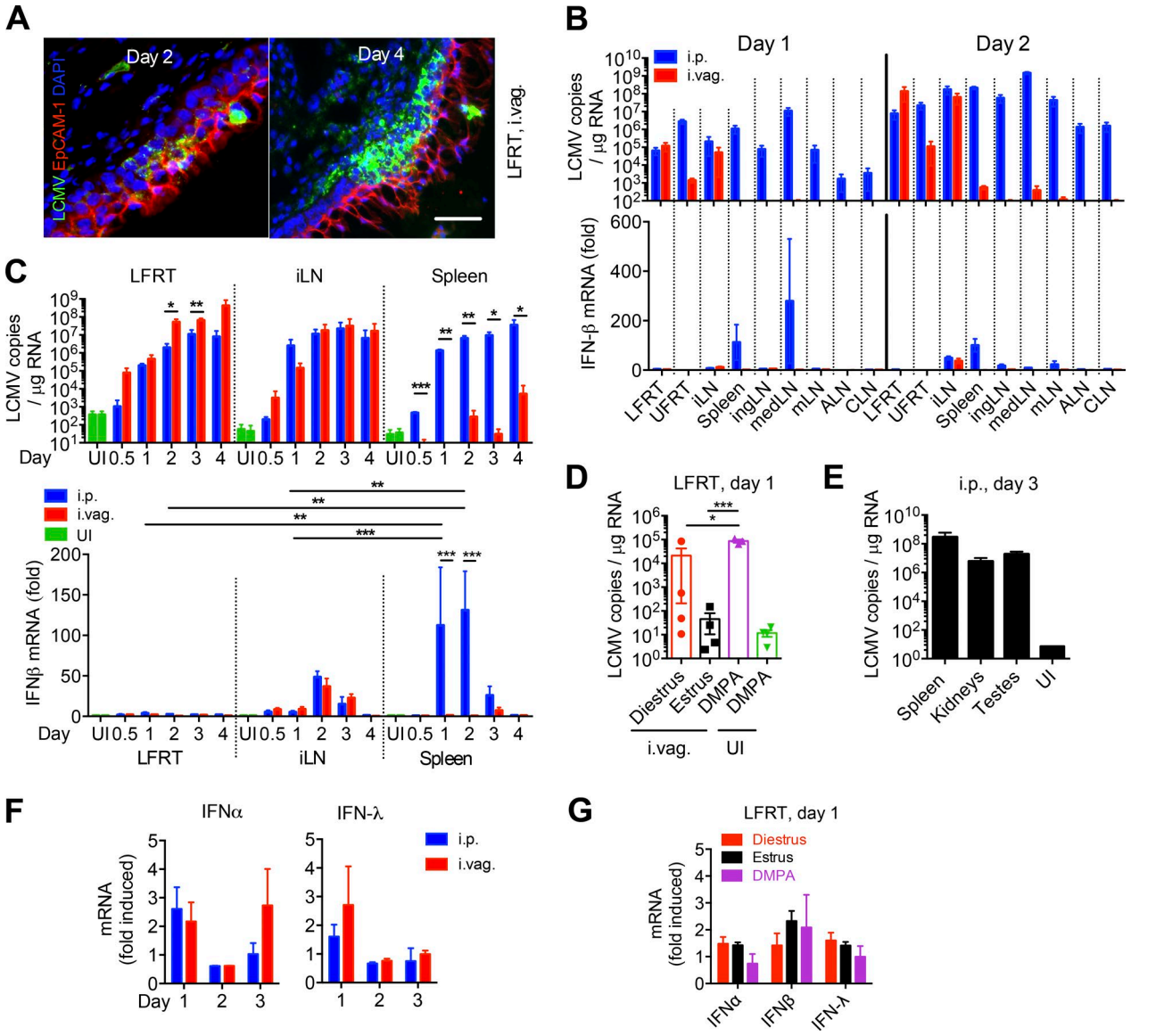

Figure 1. **Vaginally administered LCMV replicates locally with minimal induction of IFNs in the LFRT.** (A–G) Groups of C57BL/6N mice were i.p. or i.vag. infected with 2×10^5 PFU of LCMV Armstrong. (A) Immunohistochemical detection of LCMV-NP in LFRT with VL-4 monoclonal antibody 2 and 4 d after i.vag. infection. Bar, 30 µm. (B and C) LCMV copies in total RNA from the indicated tissues were determined by qRT-PCR. IFN-β mRNA levels were normalized to GAPDH and expressed as fold-change over uninfected (UI) controls. ALN, axillary LN; CLN, cervical LN; mLN, mesenteric LN. (D) Groups of female mice at the indicated stages of estrous cycle or after DMPA treatment were i.vag. infected or were left uninfected. LCMV copies were determined as in B. (E) Quantification of LCMV copies in male mice 3 d after i.p. infection. (F) IFN mRNA levels from LFRT tissues were determined as in B. (G) Levels of IFN mRNA from infected mice in D were normalized to GAPDH and expressed as fold-change over the respective group's uninfected controls. Data are represented from one (A, E, and G), two (B, D, and F), or three (C) independent experiments. $n = 3$ (A and B; days 0.5–3 LFRT and spleen in C, E, and F), 4 (D and G), or 6 (iLN and day 4 spleen in C). Error bars represent mean ± SEM. *, $P < 0.05$; **, $P < 0.01$; ***, $P < 0.001$, unpaired Student's *t* test.

IFN response is not caused by DMPA treatment of the animals. Thus, LCMV replicates robustly in the LFRT with limited induction of antiviral type I or III IFN response.

LCMV replication in the LFRT results in minimal induction of IFN signaling and inflammation

The IFN response is an important component of antiviral immunity, as it promotes the cross talk between innate and adaptive immunity. IFN produced by infected cells results in enhanced expression of type I IFN and other inflammatory cytokines in the neighboring cells, which in turn enhance maturation and antigen presentation by DCs and effector responses by T cells (Trinchieri, 2010). Although IRF-3 is constitutively expressed by most cells, IRF-7 is induced in response to IFN-α/β stimulation, and its induced expression is required to amplify the type I IFN response (Sato

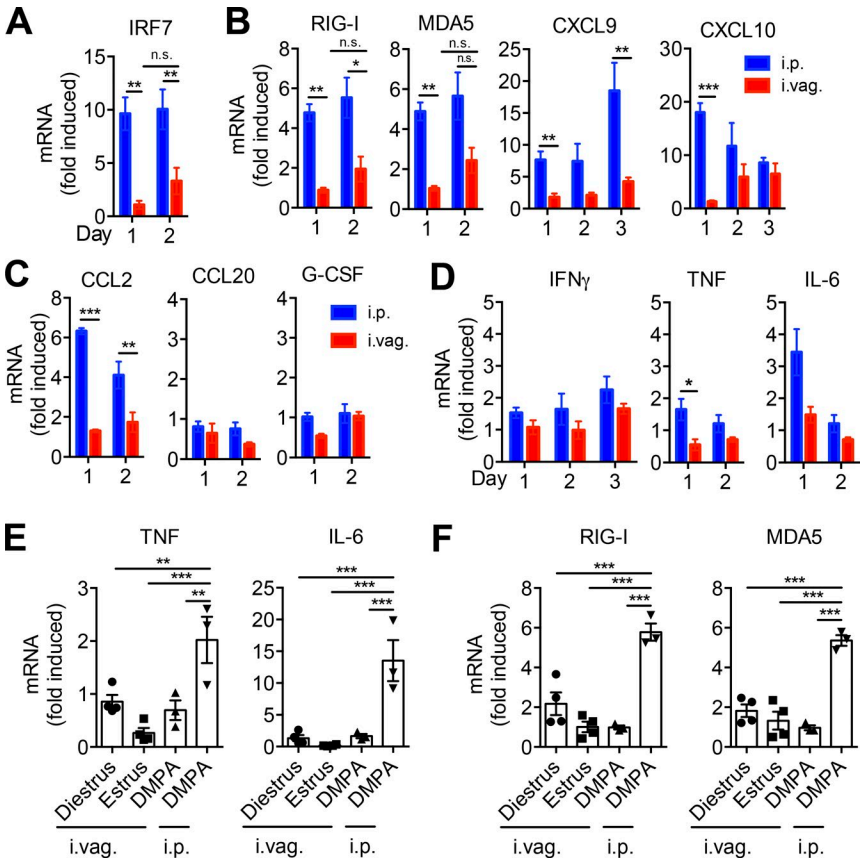

Figure 2. **Minimal induction of IFN response and inflammation in LFRT of vaginally infected mice.** (A–D) WT female mice were i.p. or i.vag. infected with 2×10^5 PFU of LCMV Armstrong. Levels of mRNA at the indicated time points were determined with qRT-PCR, normalized to GAPDH, and expressed as fold-change over uninfected controls. (E and F) Groups of female mice at the indicated stage of estrous cycle or after DMPA treatment were i.vag. infected. Levels of mRNA for the indicated cytokines or RNA sensors from the LFRT of infected mice were normalized to GAPDH and expressed as fold-change over the respective group's uninfected controls. Data are represented from three (A–D; DMPA in E and F) or one (diestrus and estrus in E and F) experiments. $n = 3$ (A; RIG-I and MDA5 in B; C; and DMPA in E and F), 4 (estrus and diestrus in E and F), or 6 (CXCL9 and CXCL10 pulled from two different experiments in B). Error bars represent mean ± SEM. *, $P < 0.05$; **, $P < 0.01$; ***, $P < 0.001$, unpaired Student's *t* test.

et al., 2000). To determine whether the induced levels of IFN-α/β were sufficient to amplify IFN signaling in infected and neighboring cells, we measured mRNA induction of IRF7 in LFRT tissue. After i.vag. LCMV infection, we observed poor IRF7 induction in the LFRT (Fig. 2 A). Interestingly however, even though we detected very low levels of type I/III IFN mRNA in the LFRT of i.p. infected animals (Fig. 1 C, bottom), IRF7 was induced ∼10-fold in the LFRT (Fig. 2 A). In i.p. infected animals, we also detected higher induction of other IFN-stimulated genes (ISGs), including RNA sensors RIG-I and MDA5 (Takeuchi and Akira, 2010) and CXCL9 and CXCL10 (Fig. 2 B), chemokines important for lymphocyte trafficking into inflamed tissues (Griffith et al., 2014), as well as those required for recruitment of monocytes (Fig. 2 C). Higher induction of various inflammatory cytokines, including IFN-γ, TNF, and IL-6, was also observed in the LFRT of i.p. but not i.vag. infected animals (Fig. 2 D). Furthermore, no significant induction of TNF, IL-6, RIG-I, and MDA5 was observed in i.vag. LCMV-infected animals that were infected during their natural diestrus stage of estrous cycle (Fig. 2, E and F), demonstrating that dampened inflammation is not caused by DMPA treatment of the animals. These data suggest that the LFRT experiences qualitatively different innate immune response after LCMV i.p. versus i.vag. infection.

Innate-mediated viral control is impaired in the LFRT after vaginal LCMV infection

To determine how limited innate immune activation affects viral control in the LFRT of i.vag. infected animals, we measured the kinetics of viral control and clearance in various tissues. At day 1 after infection, viral copy numbers are very similar in the LFRT and iLN of i.p. and i.vag. infected mice (Fig. 3, A and B). In i.p. infected animals, viral replication began to be controlled starting at day 3 after infection in both the iLN and LFRT (Fig. 3 A). In contrast, the i.vag. infected animals showed a significant delay in the kinetics of viral control in the LFRT compared with the iLN (Fig. 3 B). In fact, viral growth in LFRT of i.vag. infected animals continued exponentially until day 5 after infection, reaching ∼2-log higher than the peak of viral load in the LFRT of i.p. infected animals (Fig. 3, A and B, LFRT). Although viral dissemination to the spleen and UFRT was observed in i.vag. infected mice (Fig. 3 C), the virus was rapidly controlled in both tissues. Animals infected via either route achieved viral clearance in the LFRT by day 12 after infection (Fig. 3, A and B). Thus, after i.vag. LCMV infection, viral replication predominantly occurs in the LFRT and iLN tissues, with significantly delayed innate-mediated viral control in the LFRT.

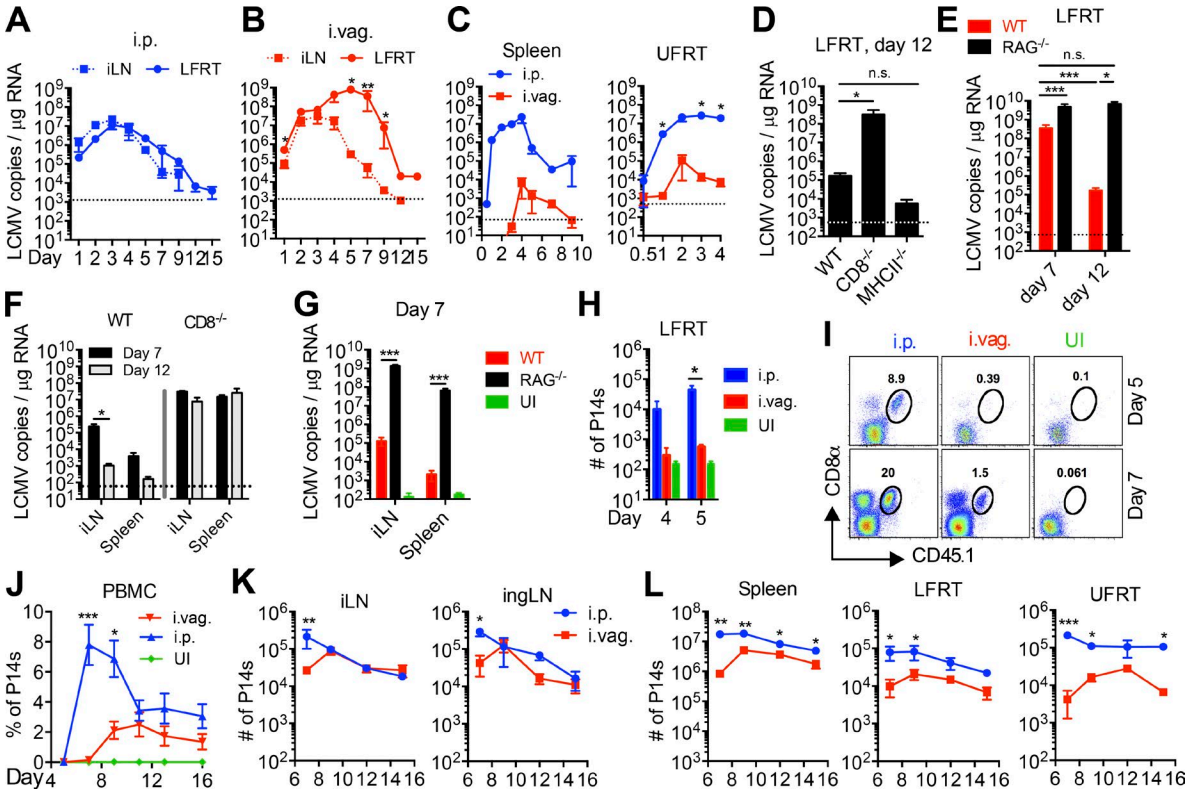

Figure 3. **Vaginal LCMV infection elicits delayed and dampened expansion of virus-specific effector CD8 T cells leading to delayed viral control in LFRT.** (A–C and H–L) Naive CD45.1$^+$ P14 CD8 T cells (P14 cells) were isolated, and 500,000 (days 0.5–4) or 20,000 (day 5 onward) P14 cells were adoptively transferred into CD45.2$^+$ WT recipient mice 1 d before i.p. or i.vag. infection with 2×10^5 PFU LCMV. (A–C) Viral copies in total RNA from the indicated tissues of infected WT mice were determined by qRT-PCR. (D–G) WT, CD8$^{-/-}$, MHC-II$^{-/-}$, or RAG1$^{-/-}$ mice were infected i.vag., and LCMV copies at the indicated times and in the indicated tissues were determined as in A–C. (H) LFRT tissues from mice in A–C were digested, and extracted immune cells were analyzed by flow cytometry. Absolute counts of P14 cells at days 4 and 5 are shown. (I) Representative flow cytometry plots showing the abundance of CD45.1$^+$ P14 cells in total cells isolated from the LFRT at days 5 and 7 after infection from P14 immune chimeras in A–C. (J) Longitudinal fraction of P14s in the PBMCs of i.p. or i.vag. infected animals. (K–L) Total number of P14s in indicated tissues at the indicated time points after i.p. or i.vag. infection. Data represent one of two (A–G and J) or three (H, I, K, and L, days 7–9) independent experiments. n = 3–4 (A–C), 10 (WT in D), 3 (CD8$^{-/-}$ in D; F; and d4 in H), 4 (MHC$^{-/-}$ in D; d5 in H; K; and L), 7 (i.p. in J), or 5 (i.vag. in J) mice per group. Error bars represent mean ± SEM. *, $P < 0.05$; **, $P < 0.01$; ***, $P < 0.001$, unpaired Student's t test. UI, uninfected.

CD8 T cells regulate viral control and clearance after vaginal LCMV infection

To determine the contribution of adaptive immunity, in particular CD8 and CD4 T cells, to LCMV control and clearance in the LFRT, we i.vag. infected WT, RAG1$^{-/-}$, CD8$^{-/-}$, and MHC-II$^{-/-}$ mice and quantitated the number of viral copies in the LFRT at day 12 after infection. Although MHC-II$^{-/-}$ and WT mice both efficiently cleared the virus, CD8$^{-/-}$ (Fig. 3 D) and RAG1$^{-/-}$ (Fig. 3 E) mice did not, which also led to systemic dissemination of LCMV after i.vag. infection (Fig. 3, F and G). These data demonstrate that CD8 T cells control and clear vaginally transmitted LCMV independently of CD4 T cells.

Next, we hypothesized that the appearance of CD8 T cells in the LFRT is required for the clearance of the virus in this tissue. We adoptively transferred congenically marked (CD45.1$^+$) P14 CD8 T cells (P14 cells), expressing a transgenic TCR that recognizes the gp33 epitope of LCMV (Pircher et al., 1990), and monitored their appearance in the LFRT of i.p. and i.vag. infected WT CD45.2 mice. Although we observed an increase in the number of host (CD8$^+$ CD45.1$^-$) and P14 cells (CD8$^+$ CD45.1$^+$) in the LFRT of i.p. infected mice as early as day 4 after infection (Fig. 3 H), we did not see an increase of P14 cells above uninfected background in i.vag. infected mice until day 7 after infection (Fig. 3 I). Thus, the appearance of CD8 T cells highly correlated with viral control in the LFRT of i.vag. infected mice. Therefore, in addition to a dampened innate immune control in the LFRT of i.vag. infected mice, the delayed appearance of virus-specific CD8 T cells further belated viral control in this tissue.

Kinetics of effector CD8 T cell expansion is delayed after vaginal LCMV infection

To further determine the kinetics and magnitude of the virus-specific CD8 T cell response, we quantified the adoptively transferred P14 cells in blood and various tissues of

i.vag. and i.p. infected mice throughout the effector and contraction phases of the T cell response. Expansion of the P14 cells was significantly slower in the peripheral blood of i.vag. versus i.p. infected mice (Fig. 3 J). Similarly, the peak of P14 cell expansion was delayed in the iLN and inguinal LN (ingLN) in i.vag. infected mice, even though the magnitude of the response was similar at later times (day 9–15) after i.p. or i.vag. infection (Fig. 3 K). The magnitude of the CD8 T cell response remained dampened in the spleen, LFRT, and UFRT at all effector time points after i.vag. infection (Fig. 3 L). Together, these data suggest that, after i.vag. infection, the delayed expansion and appearance of antigen-specific effector CD8 T cells to the LFRT contributes to the delay in adaptive-mediated viral control at later time points.

Vaginal LCMV infection delays priming of virus-specific CD8 T cells

To better understand the cause of the delayed CD8 T cell expansion after i.vag. infection with LCMV, we compared CD8 T cell priming between i.p. and i.vag. infected mice. We adoptively transferred CFSE-labeled P14 cells into WT hosts and measured CD69 and CD25 up-regulation and CFSE dilution in the transferred cells. Once the P14 cells up-regulated CD25 and down-regulated CD69 ($CD69^{lo}CD25^{hi}$), they began to proliferate (Fig. 4 A) and up-regulate CD44 (Fig. 4 B). The medLN is the primary dLN after i.p. infection (Olson et al., 2012), whereas the iLN and ingLN are the dLNs after i.vag. infection (Iwasaki, 2007; Kumamoto and Iwasaki, 2012). However, in i.vag. infected mice, priming only occurred in the iLN by day 3 after infection but not in the ingLN, medLN, or spleen (Fig. 4 C). These results are consistent with viral replication in iLNs but not in other lymphoid tissues after i.vag. LCMV infection of WT mice (Fig. 1 B).

After i.p. infection, CD69 and CD25 were up-regulated in the spleen as early as day 1 (Fig. 4 D), supported by early and robust IFN-β induction (Fig. 1 C, bottom). Even though the iLN had similar amounts of virus and IFN-β at days 1–3 after i.vag. and i.p. infection (Fig. 1 C), priming of P14 cells was slower in i.vag. versus i.p. infected mice (Fig. 4 D). Although P14 cells in the iLN were at the same stage of activation in i.p. and i.vag. infected mice at day 2, priming in i.vag. infected mice remained stalled at the $CD69^{hi}CD25^{lo}$ stage for an extra day (Fig. 4 D). This stall led to a 1-d delay in P14 cell proliferation in the iLN and an ∼2-d delay in effector P14 cells reaching the circulation, as measured by percentage of $CFSE^{lo}$ cells in the spleen (Fig. 4 E).

To determine whether a difference in the induction of inflammatory cytokines, other than IFN-β, in the iLN caused the delay in priming after i.vag. infection, we measured induction of IFN-γ and IL-6 throughout the priming phase. Surprisingly, i.vag. infected mice expressed higher levels of these cytokines in the iLN than i.p. infected mice (Fig. 4 F), suggesting that factors other than viral dose and inflammation generated in the iLN caused the 1-d delay in CD8 T cell priming after i.vag. infection.

Vaginal LCMV infection suboptimally activates Mig DCs

Next, we hypothesized that a difference in the quantity and/or quality of APCs may cause the difference in priming of CD8 T cells in the iLN at day 3 after i.p. versus i.vag. infection. Quantification of total cellularity in the iLN showed that i.vag. infected mice have larger LNs (Fig. 5 A) with a greater number of lymphocytes (Fig. 5 B) and innate cells (Fig. 5 C) than i.p. infected mice at day 3 after infection. On this day, we found that most of the DC population in the iLN of both i.p. and i.vag. infected mice comprised of migratory $CD11b^{+}$ DCs ($CD11c^{int}$ $MHC\text{-}II^{hi}$; Fig. 5, D and E; and Fig. S1, A and B). Importantly, these Mig DCs displayed higher surface expression of various activation and maturation markers in i.p. infected mice, including significantly higher levels of CD25 (Fig. 5 F). CD25 is a known maturation marker on DCs (Fukao and Koyasu, 2000; Granucci et al., 2002; Wuest et al., 2011), and its increase on DCs correlated with the expression of other classical markers of maturation, including CD40, CD86, and PD-L1 (Fig. S1, C and D). We also observed a strong correlation between CD25 expression on Mig DCs and P14 cell proliferation in the iLN of i.vag. infected mice (Fig. 5 G). Mig DCs in the iLN of i.p. infected mice showed faster maturation, as measured by the kinetics of CD25 up-regulation at days 1–4 after infection (Fig. 5 H). In particular, the difference in expression of CD25 on Mig DCs at day 3 after i.vag. versus i.p. infection paralleled the delayed priming of CD8 T cells in i.vag. mice at this time point; conversely, the sharp increase in CD25 expression on Mig DCs at day 4 after i.vag. infection corresponded with the eventual proliferation of P14 cells at this time point (Fig. 4, D and E).

We hypothesized that Mig DCs show up to the iLN in a less mature state after i.vag. infection because they do not properly mature in the LFRT because of limited induction of antiviral IFN response. We examined the maturation state of Mig DCs isolated from the LFRT at days 1–2 after infection. We did not detect differences in the number of Mig DCs in the LFRT between i.p. and i.vag. infected mice (Fig. 5 I). However, we found that Mig DCs in the LFRT of i.p. infected mice had up-regulated CD40, CD86, and PD-L1, whereas those in i.vag. infected mice resembled that of uninfected mice (Fig. 5 J). These data indicate that the delay in DC maturation begins in the LFRT, likely because of minimal induction of IFN response in this tissue after i.vag. infection (Fig. 1, C and F; and Fig. 2). Therefore, Mig DCs that migrate from the LFRT to the iLN after i.vag. infection begin their maturation process only after they reach the inflammatory environment of the iLN (Fig. 1 C and Fig. 4 F) and, hence, require more time before they are fully licensed to prime CD8 T cells (Fig. 4, D and E).

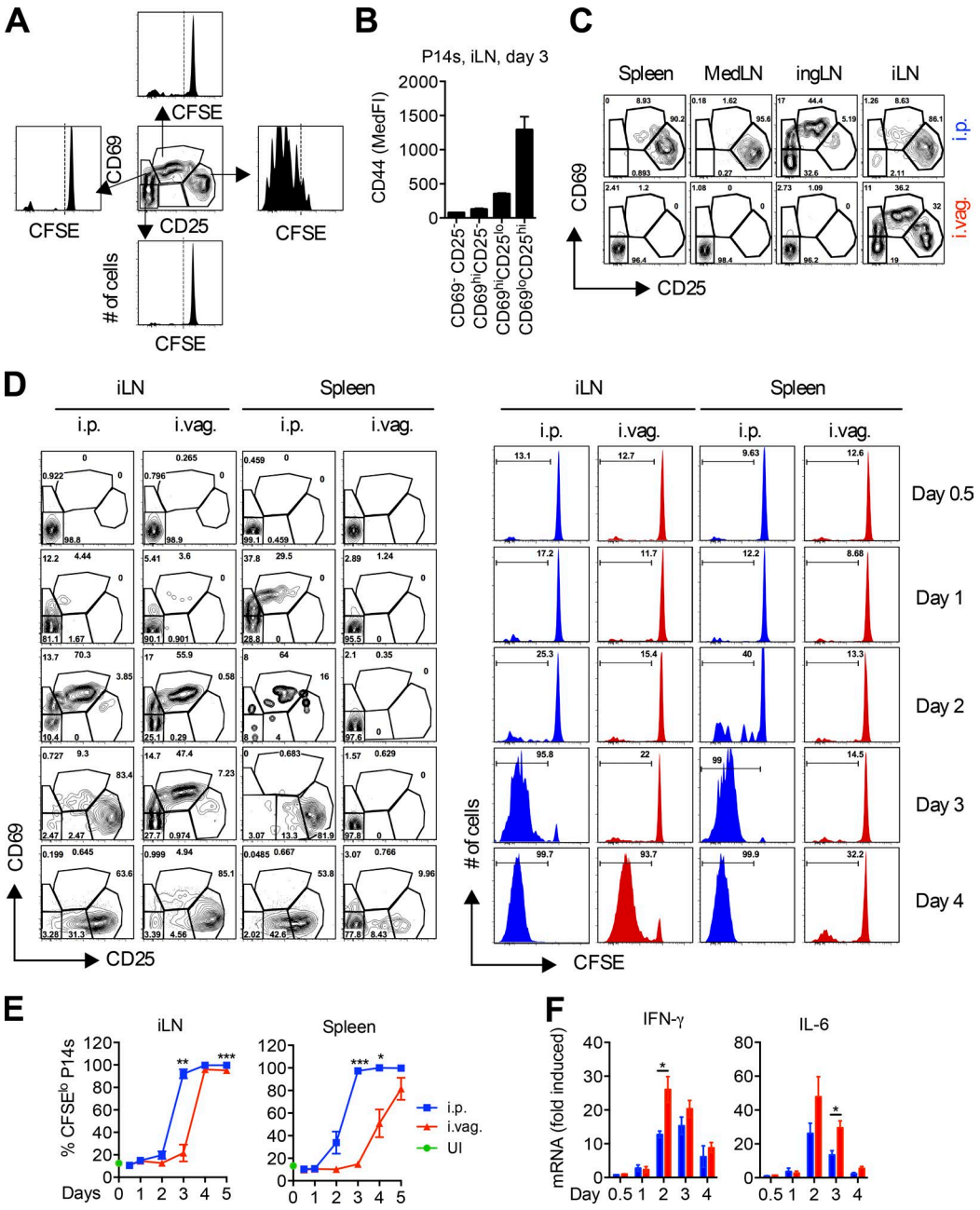

Figure 4. **Vaginal LCMV infection delays priming of virus-specific CD8 T cells.** (A–F) P14 immune chimeras were generated by adoptively transferring 500,000 CFSE-labeled CD45.1$^+$ P14 cells into naive CD45.2$^+$ B57BL/6N mice. (A) CD69 and CD25 expression patterns and CFSE dilutions of P14s in the iLN 3 d after infection. (B) CD44 expression on P14s from A. MedFI, median fluorescence intensity. (C and D) CD69 and CD25 expressions on P14 cells in the indicated tissues at day 3 (C) or the indicated days (D) after i.p. or i.vag. infection. (D) CFSE dilution of P14 cells is shown on the right. (E) Frequency of CFSE^{lo} P14 cells from D. UI, uninfected. (F) IFN-γ and IL-6 mRNA levels in iLN samples from D were measured by qRT-PCR, and their levels were normalized to GAP DH and expressed as fold-change over uninfected controls. Data are represented from one of five (D and E), three (A–C), or two (F) independent experiments. $n = 3$ (A–C; days 0–4 in E and F) or 4 (day 5 in E). Error bars represent mean ± SEM. *, $P < 0.05$; **, $P < 0.01$; ***, $P < 0.001$, unpaired Student's t test.

DC maturation and CD8 T cell priming is exceptionally delayed after vaginal LCMV transmission

Next, we wanted to determine whether the delay in DC maturation and CD8 T cell priming is unique to vaginally infected LCMV or whether it is a more general feature of mucosal and/or localized viral infection. We compared i.p. and i.vag. routes of LCMV infection with t.c. and s.c. (next to buttocks) routes of infection. Although the iLN remained the primary dLN of both t.c. and s.c. infected mice, T cell priming was also observed in the ingLN of i.p. and s.c. infected

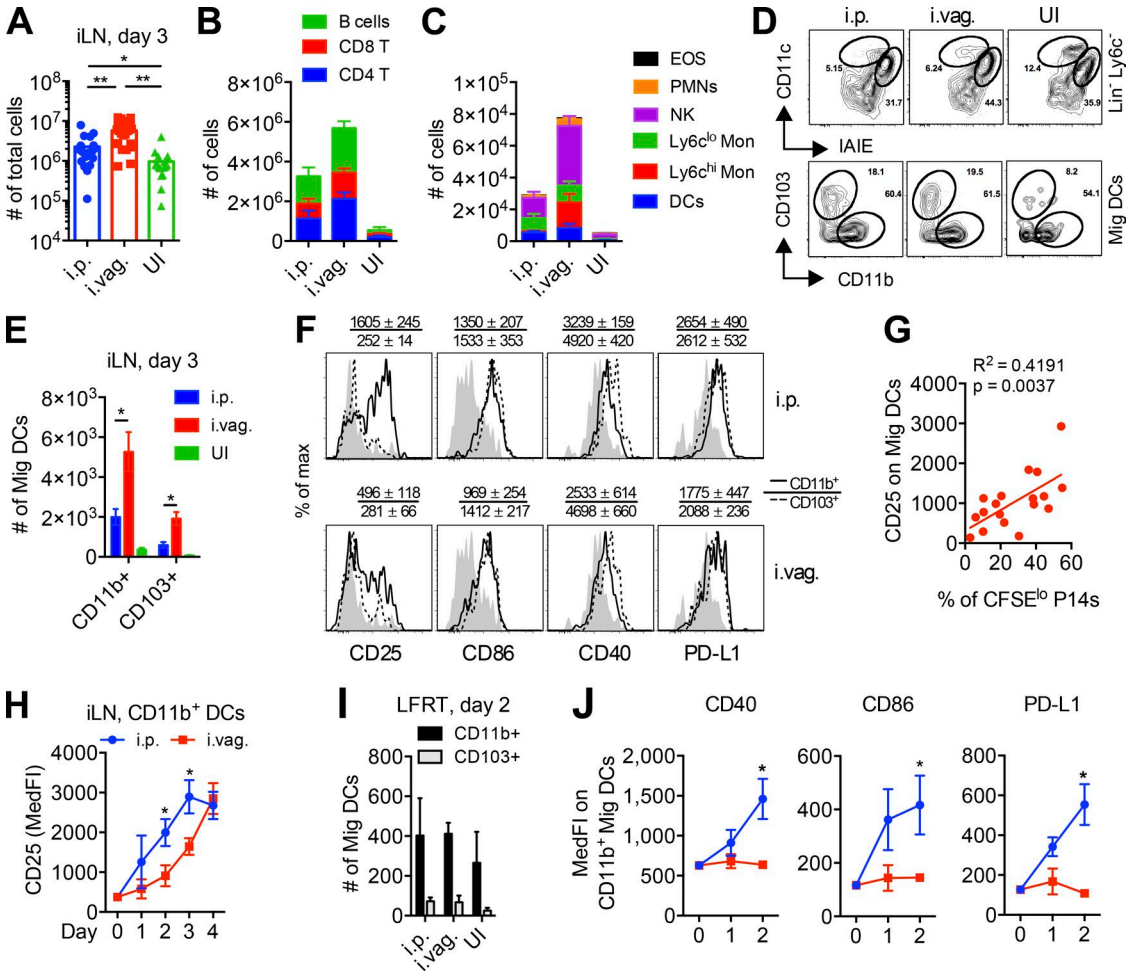

Figure 5. **Vaginal infection with LCMV elicits delayed activation of DCs.** (A–J) Female WT mice were infected either i.p. or i.vag. (A) Total cell numbers in the iLN at day 3 after infection. (B) Absolute counts of various lymphocytes in the iLN at day 3 after infection. B cells: TCRβ$^-$ CD19$^+$; CD8 T: TCRβ$^+$ CD8$^+$; CD4 T: TCRβ$^+$ CD4$^+$. (C) Absolute counts of various innate immune cells in the iLN at day 3 after infection. EOS: CD19$^-$ TCRβ$^-$ EpCAM-1$^-$ Ly6G$^-$ CD11b$^+$ Ly6c$^{int/-}$ SSC$^+$; PMNs: CD19$^-$ TCRβ$^-$ EpCAM-1$^-$ Ly6G$^+$ CD11b$^+$; NK: NK1.1$^+$; Ly6c^{lo} monocytic [Mon]: CD19$^-$ TCRβ$^-$ EpCAM-1$^-$ Ly6G$^-$ CD11b$^+$ SSC$^-$ Ly6c$^{int/-}$; Ly6c^{hi} monocytic: CD19$^-$ TCRβ$^-$ EpCAM-1$^-$ Ly6G$^-$ CD11b$^+$ SSC$^-$ Ly6c^{hi}; DCs: CD19$^-$ TCRβ$^-$ NK$^-$ Ly6G$^-$ Ly6c$^-$ MHC-II$^+$ CD11c$^+$. (D) Gating strategy showing proportion of Mig (CD11c^{int} MHC-II^{hi}) and resident (CD11c^{hi} MHC-II^{int}) DCs and CD11b and CD103 expression on Mig DCs in the iLN at day 3 after infection. IAIE, MHC-II including both I-A and I-E. (E) Absolute numbers of CD11b$^+$ and CD103$^+$ Mig DCs in iLN at day 3 after infection. (F) Representative histograms showing surface expression of activation and maturation markers on CD11b$^+$ and CD103$^+$ Mig DCs in the iLNs at day 3 after infection. The numbers above the histogram plots indicate mean ± SEM of median fluorescence intensity. Filled light-gray histograms represent Mig DCs from uninfected mice. (G) Linear correlation analysis showing association of CD25 expression on Mig DCs with CFSE dilution in P14 cells in the iLN at day 3 after i.vag. infection. (H) Kinetics of CD25 expression on CD11b$^+$ Mig DCs. (I) Numbers of Mig DCs in the LFRT at day 2 after infection. (J) Activation status of CD11b$^+$ Mig DCs at days 1–2 after infection. Day 0 represents values from uninfected mice. Data are pulled from six (A and G) or two (B, C, E, and H) independent experiments or are representative of one of five (D), three (F), or two (I and J) independent experiments. n = 18 (A), 6 (B, C, E, and H), or 3 (I and J). Error bars represent mean ± SEM. *, P < 0.05; **, P < 0.01. See also Fig. S1. MedFI, median fluorescence intensity; UI, uninfected.

mice at day 3 after infection (Fig. 6 A). P14 cell priming remained significantly delayed in the iLN of i.vag. infected mice compared with all other groups (Fig. 6, B and C), even in the presence of similar copy numbers of viral RNA in the iLNs of i.p., i.vag., and t.c. infected mice (Fig. 6 D). Intrigued by the highly significant difference in the priming of CD8 T cells after i.vag. versus t.c. infection, we hypothesized that infection of the UFRT may result in higher induction of local IFN and subsequent inflammation that leads to local maturation of APCs. Indeed, significant difference in IFN-β and IRF7 induction was detected in the FRT 24 h after t.c. versus i.vag. inoculation of LCMV, which also resulted in significantly higher induction of various inflammatory cytokines and chemokines (Fig. 6 E). Furthermore, high induction of CCL2 in t.c. infected mice correlated with higher recruitment of Ly6c^{hi} monocytes to both UFRT and LFRT tissues (Fig. 6 F), and the inflammatory environment resulted in their local activation, as measured by CD86 and CD40

up-regulation (Fig. 6 G). These higher numbers of activated $CD11b^+$ monocytic cells in FRT of t.c. infected mice contributed to an increase in the amount of activated $CD11b^+$ Mig DCs entering the iLN starting at day 1 after infection (Fig. 6, H and I), with significantly higher surface expression of CD25, CD40, and CD86 (Fig. 6 J). These data demonstrate that local induction of type I IFN and other inflammatory cytokines promotes recruitment and local maturation of monocyte-derived DCs in the FRT. Mature DCs that migrate to the draining iLN are then licensed to quickly prime CD8 T cells.

Vaginally inoculated ZIKV replicates in the LFRT of WT mice

Intrigued by the findings that innate-mediated immune control is exceptionally dampened in the LFRT of i.vag. LCMV-infected mice, we wanted to test whether this was a unique characteristic of LCMV or was also shared with other RNA viral pathogens that are sexually transmitted. High rates of sexual transmission of ZIKV have recently been reported (Brooks et al., 2016; D'Ortenzio et al., 2016), and it is known that ZIKV replication is potently inhibited by type I IFNs after systemic infection in WT animals (Grant et al., 2016; Lazear et al., 2016; Rossi et al., 2016). We therefore hypothesized that i.vag. inoculated ZIKV would elicit a similarly dampened innate immune response, allowing viral replication in the LFRT of WT animals. Thus, we i.vag. inoculated WT animals with ZIKV and measured the kinetics of viral replication over time. Using a qRT-PCR assay, we detected an about one-log increase in viral RNA copies in the LFRT at day 2 compared with day 1 after infection, demonstrating viral replication in this tissue (Fig. 7 A). Similar to LCMV, ZIKV replication in the LFRT resulted in minimal mRNA induction of type I and III IFNs (Fig. 7 B). This was also consistent with minimal and variable induction of IRF7 (Fig. 7 C), as well as various ISGs and inflammatory cytokines (Fig. 7 D), highly reminiscent of the poor innate response elicited after vaginal LCMV infection (Figs. 1 and 2). However, unlike minimal innate-mediated control of viral replication in the LFRT after i.vag. LCMV infection, the induced level of innate response seemed sufficient to begin controlling ZIKV replication by around day 3 after i.vag. infection (Fig. 7 A). Furthermore, unlike i.vag. LCMV infection, significant viral replication and ISG induction could not be detected in the iLN at day 2 after i.vag. ZIKV infection (Fig. 7, E and F). Although, similar to the LFRT tissue, we detected a positive correlation between viral RNA copies and IRF7 induction in the iLN (Fig. 7 G), suggesting that, similar to LCMV, ZIKV can also disseminate from the LFRT to the iLN. The innate-mediated antiviral response in the iLN is significantly faster and stronger than in the LFRT after LCMV i.vag. infection (Fig. 3 B); it is therefore conceivable that viral replication was strongly inhibited by a robust innate immune response as soon as ZIKV disseminated to the iLN. Interestingly, regression analyses showed that the LFRT can tolerate ∼60 times more viral load per fold-increase of IRF7 mRNA than iLN can at day 2 after i.vag. infection (Fig. 7 G). Thus, although ZIKV can replicate in the LFRT of WT animals, once disseminated to the iLN, viral replication is most likely inhibited by the elicited antiviral innate immune response. Together, these data suggest that, as ZIKV replication in WT mice is extremely sensitive to inhibition by type I IFNs, the limited induction of antiviral IFN response in LFRT, or the IFNs produced upon viral dissemination to the iLN, may be sufficient to eventually control viral replication in the vaginal mucosa.

ZIKV replication in the LFRT does not promote APC maturation

Consistent with low induction of ISGs and inflammatory cytokines (Fig. 7 D) and similar to what we had observed after i.vag. LCMV infection (Fig. 6, F and G), no signs of significant monocyte recruitment (Fig. 8, A and B) or their maturation (Fig. 8 C) were detected in the LFRT. Analysis of the draining iLN also did not reveal any significant increase in number or activation of Mig DCs in i.vag. ZIKV-infected animals (Fig. 8, D and E). Together, these data show that minimal induction of antiviral inflammation in the LFRT tissue is a common feature of both LCMV and ZIKV vaginal infection. This dampened early innate response accompanies significant viral replication in the LFRT of WT hosts without inducing APC recruitment or maturation in the vaginal mucosa.

Enhancement of inflammation in the LFRT inhibits ZIKV replication

To determine whether the enhancement of innate immune activation in LFRT would bolster ZIKV control in the LFRT of WT animals, we took two different approaches. As the first approach, we i.p. infected mice with LCMV, knowing that this route of LCMV infection generates significant antiviral IFN response and inflammation in the LFRT (Fig. 2), followed by i.vag. inoculation with ZIKV the next day. As hypothesized, we found that animals that were i.p. LCMV infected were able to completely inhibit ZIKV replication in the LFRT (Fig. 9 A). This strikingly high level of protection correlated with significantly induced mRNA levels of various ISGs, including RIG-I, MDA5, and IRF7 (Fig. 9 B), as well as expected activation of Mig DCs in the iLN (Fig. 9 C).

The second approach we took to enhance antiviral innate immunity in the LFRT was to vaginally administer acitretin, which is a derivative of retinoic acid that enhances RIG-I signaling (Li et al., 2016). Vaginal treatment with acitretin transiently induced the expression of RIG-I and MDA5 in the LFRT within 2 h of treatment (Fig. 9 D), which was followed by transient mRNA induction of type I and III IFNs (Fig. 9 E) as well as inflammatory cytokines IL-6 and TNF (Fig. 9 F). Next, we treated the animals vaginally with acitretin 1 d before (−D1) i.vag. ZIKV inoculation. Strikingly, animals vaginally pretreated with acitretin lacked any detectable viral replication in the LFRT tissue (Fig. 9 G). Together, these data show that low level of IFNs and inflammation that is naturally generated by ZIKV in the LFRT is insufficient to inhibit early viral replication, prolonging localized viral persistence in WT animals.

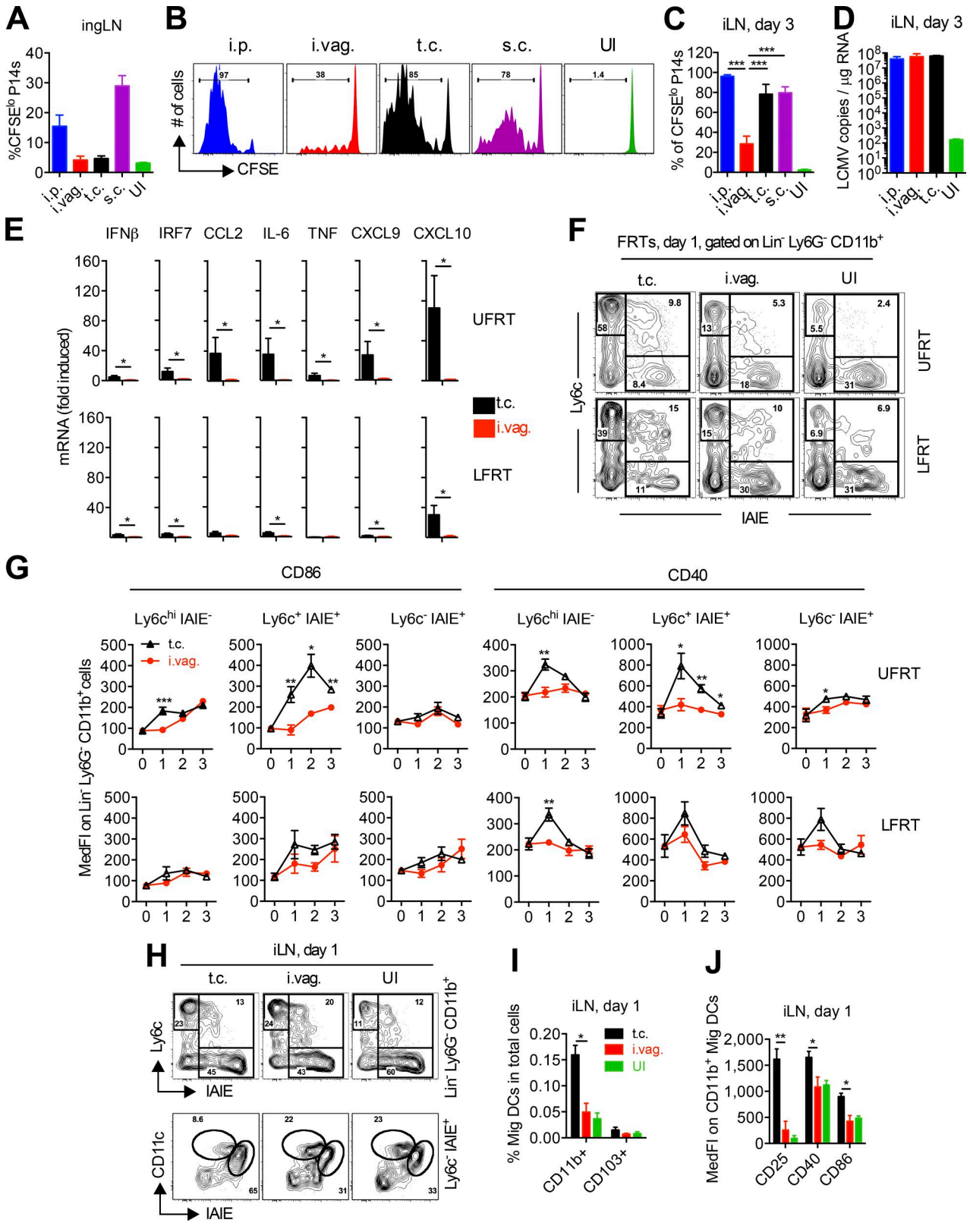

Figure 6. **Delay in innate and adaptive immune activation is not common to all mucosal or local infections.** (A–J) P14 immune chimeras were generated by adoptively transferring 500,000 CFSE-labeled CD45.1⁺ P14 cells into naive female CD45.2⁺ B57BL/6 mice. (A) CFSE dilution of P14 T cells in ingLN at day 3 after infection with LCMV via the indicated routes. (B) Representative histogram plots showing CFSE dilution of P14 cells in the iLN at day

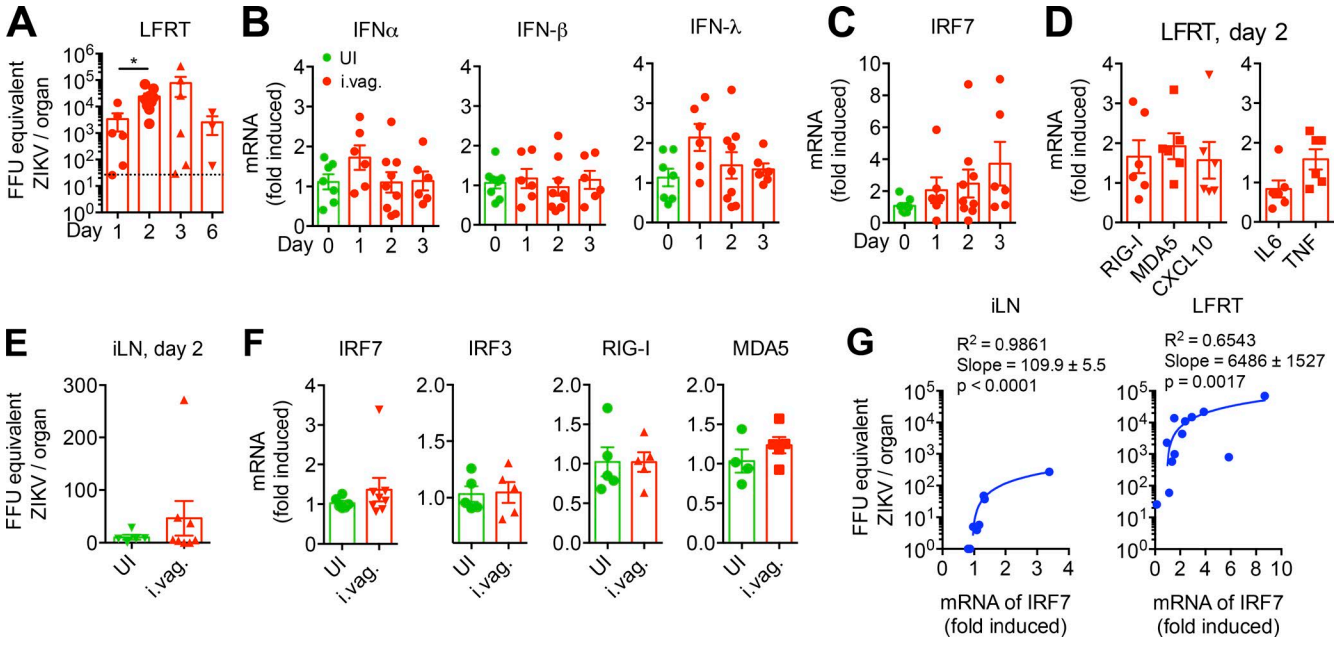

Figure 7. **Vaginally inoculated ZIKV replicates in the LFRT of WT mice with minimal induction of IFN response.** (A–G) Groups of C57BL/6N female mice were i.vag. infected with 2×10^4 FFU of ZIKV (PRVABC59). (A) FFU equivalent of ZIKV in total RNA from LFRT tissues was determined by qRT-PCR at the indicated time points after infection. (B–D) Levels of mRNA for the indicated genes from LFRT were determined from total RNA using qRT-PCR, normalized to GAPDH, and expressed as fold-change over uninfected controls. (E and F) Viral load or ISGs from iLN at day 2 after infection were determined as in A and B–D. (G) Linear regression analysis of FFU equivalent of ZIKV and induced IRF7 in the iLN and LFRT tissues after i.vag. infection. Each dot represents one mouse. n = 3–6 pulled from two independent experiments. Data represent mean ± SEM. *, $P < 0.05$. UI, uninfected.

DISCUSSION

In this study, we show that upon LCMV or ZIKV vaginal exposure, antiviral IFN response and inflammation is minimally induced in the LFRT, providing a window of opportunity for these pathogens to replicate in the vaginal mucosa. Significantly, the rescue of the dampened innate immune response in the LFRT, either by systemic infection with an unrelated pathogen or vaginal administration of acitretin, resulted in inhibition of ZIKV replication. These data suggest that the natural innate immune response that is elicited in response to ZIKV and LCMV after vaginal inoculation is not sufficient to control early viral replication in the LFRT. Furthermore, using LCMV, we show that the dampened innate immune response can also delay the formation of an antiviral adaptive immune response after i.vag. infection.

Limited induction of antiviral immunity, including type I/III IFNs, is not a common feature of all vaginal viral infections, as vaginal HSV-2 infection in mice results in induction of type I and III IFNs (Iversen et al., 2016; Oh et al., 2016) as well as recruitment of DCs to the vaginal mucosa that are crucial for initiation of the protective T cell response (Zhao et al., 2003). Interestingly however, although vaginal treatment with either TLR3/RIG-I–like receptors agonist polyinosinic:polycytidylic acid (poly[I:C]) or TLR9 agonist CpG-oligodeoxynucleotide (CpG-ODN) provides protection against vaginal HSV-2 infection, vaginal poly(I:C) treatment causes little or no inflammation compared with CpG-ODN treatment (Ashkar et al., 2004; Gill et al., 2006). Similarly, although single vaginal treatment with CpG-ODN results in local and peripheral organ enlargement, repetitive

3 after infection. (C) Percentages of the CFSE-diluted fraction in P14 cells from B. (D) Quantification of LCMV copies by qRT-PCR from total RNA of iLN. (E) mRNA levels for the indicated genes were determined from total RNA using qRT-PCR, normalized to GAPDH, and expressed as fold-change over uninfected controls. (F) Representative flow cytometry plots showing enrichment of monocytes in the UFRT or LFRT tissue 1 d after i.vag. or t.c. infection. Cells were gated on Lineage$^-$ (Lin$^-$; CD19$^-$ TCRβ$^-$ NK1.1$^-$) Ly6G$^-$ CD11b$^+$. (G) Activation kinetics of CD11b$^+$ populations from D in LFRT and UFRT after i.vag. or t.c. infection. The values at day 0 are from uninfected mice. (H) Flow cytometry plots showing enrichment of monocytes (top) and the proportion of Mig and resident DCs within the Ly6c$^-$ MHC-II$^+$ gate (bottom) in the iLN 1 d after i.vag. or t.c. infection. (I) Fraction of Mig DCs in the iLN 1 d after i.vag. or t.c. infection. (J) Activation state of CD11b$^+$ Mig DCs in the iLN 1 d after i.vag. or t.c. infection. Data represent one of five (i.p. and i.vag. in A–D), four (t.c. in B and C), or two (D; t.c. in E–J) independent experiments. Data for i.vag. in E, G, I, and J were pulled from two independent experiments. n = 3 (A–D), 4 (t.c. in E–J), or 6 (i.vag. in E–J). Error bars represent mean ± SEM. *, $P < 0.05$; **, $P < 0.01$; ***, $P < 0.001$, unpaired Student's t test. IAIE, MHC-II including both I-A and I-E; MedFI, median fluorescence intensity; UI, uninfected.

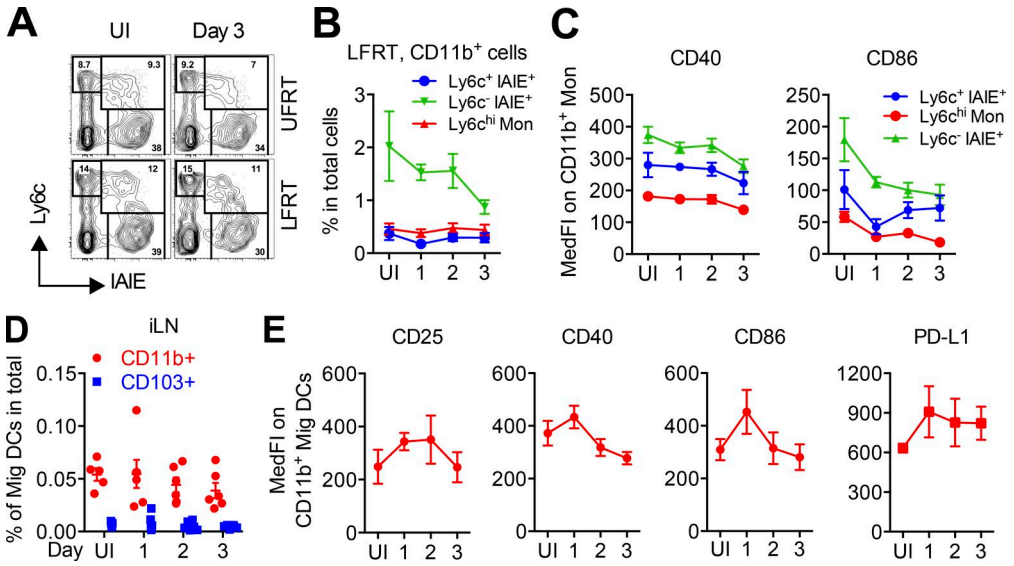

Figure 8. **Vaginally inoculated ZIKV induces minimal APC recruitment and activation.** (A–E) Groups of C57BL/6N female mice were i.vag. infected with 2×10^4 FFU of ZIKV (PRVABC59). (A) Representative flow cytometry plots showing CD11b$^+$ monocytic cells in the UFRT or LFRT tissues of uninfected mice or 3 d after i.vag. ZIKV infection. Cells were gated on Lineage$^-$ (CD19$^-$ TCRβ$^-$ NK1.1$^-$) Ly6G$^-$ CD11b$^+$. (B) Percentages of different subsets of monocytic (Mon) cells in LFRT of i.vag. infected mice among total cells at the indicated days. (C) Surface expression of activation markers on different monocytic populations in A and B. (D) Percentages of different subsets of Mig DCs among total cells in iLN of i.vag. infected mice at the indicated days after infection. (E) Surface expression of the indicated activation markers on CD11b$^+$ Mig DCs in D. $n = 6$ pulled from two independent experiments. Data represent mean ± SEM. IAIE, MHC-II including both I-A and I-E; MedFI, median fluorescence intensity; UI, uninfected.

i.vag. treatment with poly(I:C) does not generate the same effect (Herbst-Kralovetz and Pyles, 2006). Furthermore, when mice were i.vag. treated with poly(I:C), CpG-ODN, or TLR7 agonist imiquimod, only CpG-ODN promoted recruitment of CD11c$^+$ DCs to the vaginal mucosa and strongly up-regulated MHC-I expression on both leukocytes and epithelial cells, whereas imiquimod and poly(I:C) induced weak up-regulation of MHC-I only on the epithelium and not in the lamina propria (Nurkkala et al., 2007). CpG-ODN was also the strongest stimuli for chemokine production, and CCL3 production remained highly elevated in CpG-ODN–treated animals for up to 7 d after the treatment, whereas it waned quickly in animals treated with imiquimod and poly(I:C) (Nurkkala et al., 2007). Collectively, these studies suggest that DNA ligands have a stronger inflammatory effect on the vaginal mucosa, and sensing of CpG-ODN results in recruitment of professional APCs to the vaginal mucosa, whereas the same effect is not seen with RNA ligands. These studies indeed support our findings where we show for the first time that vaginal infection with two different RNA viral pathogens does not result in significant induction of type I/III IFNs or recruitment and activation of APCs in the vaginal mucosa.

Furthermore, in a recent study that examined early immune response after i.vag. simian immunodeficiency virus infection in nonhuman primates, despite ample viral replication in the vaginal tissue at day 1 after infection, an absence of induced antiviral genes, including IFN-stimulated restriction factors, was observed. However, the induction of these genes was observed during peak systemic viral replication (Barouch et al., 2016), suggesting that an IFN response is elicited only once virus disseminates to peripheral tissues. In accordance with these findings, we also detected very limited induction of type I IFN and various ISGs in the LFRT tissue after i.vag. LCMV or ZIKV infection, whereas systemic i.p. infection with LCMV resulted in enhanced expression of various ISGs in the LFRT, which were sufficient to inhibit ZIKV replication in this tissue. Therefore, the qualitative difference in innate immune activation in the LFRT after i.vag. versus i.p. routes of infection is most likely related to the robust pool of IFNs that is generated after systemic infection, which results in induction of global ISGs in all tissues, including the LFRT. These findings suggest that the natural innate response that is elicited by these RNA viral pathogens upon vaginal exposure is too dampened to provide rapid control of viral replication, which ultimately results in high viral titers in this tissue. It will be important to further determine the biological reasons and the exact mechanism causing this dampened innate immune activation against vaginally inoculated RNA viral pathogens.

In contrast to the LFRT, once LCMV and ZIKV disseminate to the draining iLN, UFRT, or the spleen, the host rapidly elicits a protective immune response. We also detected a much stronger innate and faster adaptive immune response if LCMV was directly inoculated into the UFRT as compared with i.vag. infection of the LFRT. This comparison suggests that the dampened innate response in the LFRT, which

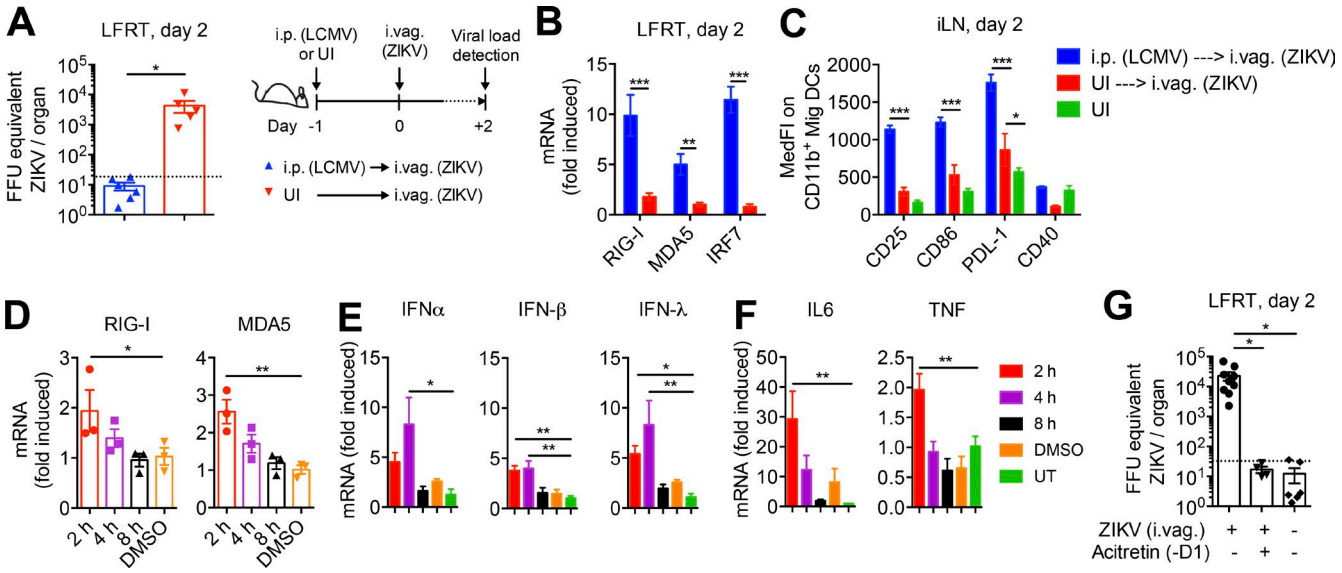

Figure 9. **Systemic or local induction of IFN response prevents vaginal ZIKV infection.** (A) WT mice were i.p. infected with 2×10^5 PFU of LCMV or were left uninfected, followed by i.vag. inoculation with 2×10^4 FFU of ZIKV the next day. LFRT tissues were collected 2 d after i.vag. ZIKV inoculation and analyzed by qRT-PCR for ZIKV load. The dotted line indicates the level of detection. (B) Levels of mRNA for the indicated genes were determined by qRT-PCR from LFRT samples in A, normalized to GAPDH, and expressed as fold-increase over uninfected controls. (C) Surface expression of activation markers on $CD11b^+$ Mig DCs in iLN of mice in A and B. (D–F) Mice were vaginally treated with 20 µl of 2 mM acitretin in DMSO, and LFRT tissues were collected at the indicated time points after treatment. Levels of mRNA were detected as in B. (G) Groups of mice were vaginally treated with 20 µl of 2 mM acitretin 1 d before (−D1) i.vag. inoculation with ZIKV, were untreated but infected, or were left uninfected. Viral load in the LFRT tissues was determined as in A 2 d after infection. (A–C) Data are represented from two independent experiments. (D–G) The acitretin treatment results are represented from two separate experiments. $n = 3$ (D–F), 4–9 (G), or 5–6 (A–C). Error bars represent mean ± SEM. *, $P < 0.05$; **, $P < 0.01$; ***, $P < 0.001$. MedFI, median fluorescence intensity; UI, uninfected; UT, untreated.

also results in a delayed adaptive immune activation, is an exceptional feature of the vaginal mucosa that is not shared at least with this other relevant mucosal route of infection. As the UFRT and LFRT have different composition of resident innate and adaptive cells (Wira et al., 2015), it will also be important to further investigate the exact mechanism by which the LFRT and the UFRT differentially elicit an antiviral response against RNA viral pathogens.

Vaginal treatment with acitretin transiently induced mRNA expression of RIG-I and MDA5 in the LFRT, followed by mRNA induction of type I/III IFNs and other inflammatory cytokines. Importantly, vaginal pretreatment with acitretin inhibited ZIKV replication in the LFRT of WT mice. These results provide conceptual proof that induction of the RIG-I pathway may provide an attractive option for treating vaginal ZIKV infections. Although acitretin has never been administered vaginally, oral therapeutic administration for psoriasis in pregnant women is known to cause fetal abnormalities (Yiu et al., 2015). Therefore, it will be important to investigate whether RIG-I–inducing drugs other than acitretin would have similar effects in terms of inhibiting vaginal ZIKV infection as well as their propensity to cause fetal abnormalities.

Our findings also suggest that protective immunity may be dampened and/or delayed during vaginal ZIKV transmission compared with the immune response that is elicited upon systemic spread of the virus through mosquito bites. Importantly, these findings may have critical implications for fetal infection and abnormalities observed upon ZIKV infection (Lessler et al., 2016). During pregnancy, multiple mechanisms originating from both mother and fetus contribute to the development and maintenance of tolerance (Munoz-Suano et al., 2011; Warning et al., 2011; Erlebacher, 2013), which may further dampen induction of IFNs in both the LFRT and UFRT and favor replication of sexually transmitted ZIKV and potential dissemination to the fetal compartment and infection of the fetus, as was recently also experimentally demonstrated (Yockey et al., 2016).

As we currently lack a suitable small-animal model for studying how innate and adaptive immunity are elicited against vaginally transmitted RNA viruses, development of such relevant models and their validation is important toward gaining the knowledge required to successfully prevent or treat sexually transmitted infections with this class of pathogens. To this end, our study provides the first mouse models to study vaginal transmission of RNA viral pathogens and contributes insight into the plausible mechanism by which the LFRT supports their replication. Our i.vag. ZIKV model will permit rapid preclinical testing of various microbicides and their safety and efficacy to inhibit ZIKV replication at a relevant site of high viral replication in vivo. Furthermore,

because LCMV has evolved with its natural mouse host and already serves as an excellent model pathogen to study antiviral CTL immunity, studying i.vag. LCMV will support modeling both the innate and the CD8 T cell–mediated immune responses that are elicited after vaginal transmission of RNA viral pathogens. As such, future i.vag. LCMV studies will foster a better understanding of how a dampened and localized innate immune response may affect the establishment of protective immunity in the LFRT, knowledge needed to develop protective vaccines against current and emerging RNA viral pathogens.

MATERIALS AND METHODS

Mice

C57BL/6NCr CD45.2$^+$ WT (NCI), B6-Ly5.1/Cr CD45.1$^+$ (NCI), Rag1^{tm1Mom} (Mombaerts et al., 1992), and Tg(TcrLCMV)327Sdz (Pircher et al., 1990) mice crossed to CD45.1, Rag1$^{-/-}$, H2$^{dlAb1\text{-}Ea}$ (The Jackson Laboratory; Madsen et al., 1999), and Cd8a^{tm1Mak} (The Jackson Laboratory; Fung-Leung et al., 1991) mice were used in this study. Mice were housed and bred in the Gladstone Institutes' animal facility. Female mice (8–20 wk old) were used throughout this study, except where indicated. Age-matched animals were assigned to various treatment groups blindly. All animal experiments were conducted in accordance with guidelines set by the Institutional Animal Care and Use Committee of the University of California, San Francisco.

Adoptive transfer of T cells and viral infection

Unless stated otherwise, all female mice in all infection groups or uninfected group were injected s.c. with Depo-Provera (GE Healthcare) at 1 mg per mouse in a 200-µl volume, 7 d before infection. To determine the stage of natural estrous cycle, animals were examined visually for vaginal inflammation, and daily vaginal smears were also collected by gentle lavage with 50 µl of sterile PBS using a sterile 200-µl pipetted tip. Stage of estrous cycle was confirmed by examining the proportion and morphology of leukocytes and epithelial cells present under a light microscope (Byers et al., 2012). Animals were followed for a minimum of two cycles, and those who did not have normal 4–5 d cycles were not used in this study. P14 chimeras for effector phase experiments were generated by adoptive transfer of ∼2 × 10^4 naive CD45.1$^+$ P14 CD8$^+$ T cells (P14 cells) on a RAG$^{-/-}$ background into CD45.2$^+$ congenic WT recipient mice. For priming experiments, P14 cells were labeled with 0.25 µM CFSE (Molecular Probes) at 37°C for 10 min, and ∼5 × 10^5 cells were transferred into each recipient mouse via retroorbital injection. 1 d later, mice were infected with 2 × 10^5 PFU of LCMV$_{Arm}$ via i.vag., i.p., t.c, or s.c. route. Experiments were performed with two batches of LCMV, with similar results. ZIKV strain PRV ABC59 (Puerto Rico; 2015) was purchased from the ATCC (VR-1843). Stocks of ZIKV were propagated in Vero cells (CCL-81; ATCC), and viral titers were determined by focus-forming assay on LLC-MK2 cells (CCL-7; ATCC). For i.vag. infection, mice were anesthetized using isoflurane, and 20 µl of viral suspension was inoculated into the vaginal cavity using a p200 micropipette, without causing abrasion. For t.c. infections, the same volume of LCMV$_{Arm}$ was inoculated into one arm of the uterus using a gel-loading tip through a cut-off end of a P-200 pipet tip as a speculum, without causing any tissue damage. The same dose of the virus in a 100-µl suspension was injected s.c. into the buttock next to the rectal opening.

Acitretin treatment

After 6 d of treatment with 1 mg/mouse Depo-provera, 20 µl of 2 mM acitretin (Sigma-Aldrich) in DMSO (Hsia et al., 2008) was administered into the vaginal cavity at the indicated times either before or after i.vag. ZIKV inoculation. All mice were anesthetized in an isoflurane chamber before administering the drug.

Isolation of immune cells and flow cytometry

LN and spleen tissues were processed into single-cell suspensions. The vagina was separated from the urethra and cervix. The LFRT consisted of vaginal tissue and the transformation zone. LFRT or UFRT tissues from groups of mice (one to three mice per group) were digested in 1 mg/ml collagenase type IV (Worthington Biochemical Corporation) and 75 µg/ml DNase I (Roche) in RPMI medium. Single-cell suspensions were obtained from the digested tissues using GentleMACS Dissociator (Miltenyi Biotec) according to the manufacturer's protocol. For isolation of DC populations, 100 units/ml of hyaluronidase (Sigma-Aldrich) was combined with collagenase IV and DNase I. Cell counts were obtained using an Accuri cytometer (BD), and cell numbers were normalized before antibody surface staining.

After blocking Fc receptors with anti-CD16/CD32, single-cell suspensions were incubated with a mixture of fluorescence-conjugated anti–mouse antibodies for 30 min at 4°C. Stained cells were washed once and acquired with an LSR II flow cytometer and FACSDiva software (BD). AF700 CD8α (YTS169.4), PE-Cy7 CD8α (SK1), Percp-Cy5.5 CD45.1 (A20), AF700 IAIE (MHC-II; M5/114.15.2), PE-Cy7 Ly6c (HK1.4), biotin EpCAM-1 (epithelial cell adhesion molecule 1; G8.8), and APC-Cy7 CD11c (N418) antibodies were from BioLegend. BV421 CD40 (3/23), PE PD-L1 (MIH5), PE-CF594 Ly6G (1A8), PerCP-Cy5.5 CD11b (M1/70), BV605 CD44 (IM7), BV605 CD86 (GL-1), BV650 NK1.1 (PK136), PE-CF594 CD25 (PC61), APC-Cy7 TCRβ (H57-597), BV510 CD69 (H1.2F3), BV510 CD103 (M290), and biotin-conjugated NK1.1 (PK136) and TCRβ (H57-597) antibodies were from BD. AF488 CD25 (PC-61) and biotin-conjugated CD19 (1D3) antibodies were from the University of California, San Francisco Monoclonal Antibody Core.

Immunohistology of LFRT tissues

For immunofluorescence staining, 4% paraformaldehyde-fixed cryosections were treated with 1% SDS, blocked with Tris-NaCl–blocking (TNB) buffer (Tyramide Signal

Amplification kit; PerkinElmer) supplemented with 5% donkey serum, and stained with a rat monoclonal antibody (VL4) against LCMV-nucleoprotein (LCMV-NP; Bio X Cell). After neutralizing endogenous peroxidase with 3% H_2O_2, sections were incubated with horseradish-peroxidase–coupled donkey anti–rat immunoglobulin (Jackson ImmunoResearch Laboratories, Inc.). Epithelial cells were detected using an A647-conjugated monoclonal antibody (BioLegend) against EpCAM-1. LCMV-NP was visualized by incubating sections with tyramide-Cy3 (Tyramide Signal Amplification kit; Perkin Elmer). DNA/nuclei were visualized using DAPI. As negative controls, sections were stained without incubation with a primary antibody. Stained sections were observed by fluorescence microscopy (Axiovert 200 inverted microscope; ZEISS). Green, red, and blue channel images were merged with AxioVision 4.8 software. Images were enhanced for color contrast using Photoshop CS2 software (Adobe).

RNA isolation and quantitative real-time PCR

Isolated FRT tissues were chopped into small pieces, collected in TRIzol tubes filled with 3 mm of zirconium beads, and homogenized in three 10-s pulses using a Beadbug microtube homogenizer (Benchmark Scientific). RNA was isolated with TRIzol reagent according to the manufacturer's instructions (Invitrogen). 1–5 µg RNA was reverse transcribed into cDNA with a Maxima First Strand cDNA Synthesis kit with dsDNase (Thermo Fisher Scientific). Real-time PCR was performed using 2x SensiFAST probe Hi-Rox mix (Bioline) with gene-specific primers (Table S1) and run on an ABIPrism 7900 sequence detector with the ΔΔCt method from SDS 2.4 software (Applied Biosystems). The relative expression of genes was calculated with the formula $2^{-\Delta Ct}$, where ΔCt = Ct target gene − Ct endogenous control gene. *Gapdh* was used as the endogenous control housekeeping gene. Viral burden was determined from a standard curve produced using serial 10-fold dilutions of ZIKV RNA or LCMV plasmid.

Statistical analysis

Prism 6.0 (GraphPad Software) was used for data analysis. Statistical significance was determined by two-tailed Student's *t* test for two groups. All experimental data were included in the statistical analyses. Analyses with a P-value ≤0.05 were considered statistically significant. For linear regression analysis, the linear model was fit using focus-forming units (FFU) without log, and the log-10 presentation is for visualization.

Online supplemental material

Fig. S1 shows gating strategy and maturation of Mig DCs in the iLN of LCMV-infected animals. Table S1 lists the primer sequences used for qRT-PCR reactions used in this study.

ACKNOWLEDGMENTS

We thank M. Matloubian for $LCMV_{Arm}$ stock and propagation protocols, J. Luong for help with maintaining the mouse colonies, and F. Wu for technical assistance. We are grateful to J. Cyster (University of California, San Francisco [UCSF]), M. Matloubian (UCSF), W. Greene (Gladstone Institute of Virology and Immunology/UCSF), and M. R. Jakobsen (Aarhus University) for critical reading of the manuscript and to G. Howard and C. Herron (Gladstone) for editorial assistance. This publication was made possible with help from the UCSF-Gladstone Institutes CFAR, an NIH-funded program (P30 AI027763) supporting Gladstone's flow core. The Gladstone Institutes received support for its animal care facility from a National Center for Research Resources grant (RR18928).

This work was supported by grants from the National Institutes of Health (NIH; DP2 AI112244), a University of California Hellman Award, a Center for AIDS Research (CFAR) Pilot Award (P30 AI027763 and CNIHR P30 AI027767 to S. Sanjabi), a California Institute for Regenerative Medicine/Gladstone Institutes Fellowship (TG2-01160), a CFAR Mentored Scientist Award (P30 AI027763 to S. Khan), and a grant from the NIH (R01 AI097552 to M. Ott).

The authors declare no competing financial interests.

Author contributions: conceptualization, S. Sanjabi and S. Khan; methodology, S. Khan, A. Ezaki, and S. Sanjabi; formal analysis, S. Khan; investigation, S. Khan., E.M. Woodruff, M. Trapecar, and T.C. Borbet; resources, M. Ott and K.A. Fontaine; writing (original draft), S. Sanjabi and S. Khan; writing (review and editing), S. Sanjabi, S. Khan, M. Trapecar, M. Ott, and K.A. Fontaine; visualization, S. Khan and S. Sanjabi; supervision, S. Sanjabi and S. Khan; and funding acquisition, S. Sanjabi and M. Ott.

Submitted: 8 August 2016
Revised: 17 September 2016
Accepted: 17 October 2016

REFERENCES

Ashkar, A.A., X.D. Yao, N. Gill, D. Sajic, A.J. Patrick, and K.L. Rosenthal. 2004. Toll-like receptor (TLR)-3, but not TLR4, agonist protects against genital herpes infection in the absence of inflammation seen with CpG DNA. *J. Infect. Dis.* 190:1841–1849. http://dx.doi.org/10.1086/425079

Barouch, D.H., K. Ghneim, W.J. Bosche, Y. Li, B. Berkemeier, M. Hull, S. Bhattacharyya, M. Cameron, J. Liu, K. Smith, et al. 2016. Rapid inflammasome activation following mucosal SIV infection of Rhesus monkeys. *Cell.* 165:656–667. http://dx.doi.org/10.1016/j.cell.2016.03.021

Barton, L.L., M.B. Mets, and C.L. Beauchamp. 2002. Lymphocytic choriomeningitis virus: emerging fetal teratogen. *Am. J. Obstet. Gynecol.* 187:1715–1716. http://dx.doi.org/10.1067/mob.2002.126297

Belkaid, Y., and S. Naik. 2013. Compartmentalized and systemic control of tissue immunity by commensals. *Nat. Immunol.* 14:646–653. http://dx.doi.org/10.1038/ni.2604

Black, C.A., L.C. Rohan, M. Cost, S.C. Watkins, R. Draviam, S. Alber, and R.P. Edwards. 2000. Vaginal mucosa serves as an inductive site for tolerance. *J. Immunol.* 165:5077–5083. http://dx.doi.org/10.4049/jimmunol.165.9.5077

Brooks, J.T., A. Friedman, R.E. Kachur, M. LaFlam, P.J. Peters, and D.J. Jamieson. 2016. Update: Interim guidance for prevention of sexual transmission of Zika virus – United States, July 2016. *MMWR Morb. Mortal. Wkly. Rep.* 65:745–747. http://dx.doi.org/10.15585/mmwr.mm6529e2

Byers, S.L., M.V. Wiles, S.L. Dunn, and R.A. Taft. 2012. Mouse estrous cycle identification tool and images. *PLoS One.* 7:e35538. http://dx.doi.org/10.1371/journal.pone.0035538

Casey, K.A., K.A. Fraser, J.M. Schenkel, A. Moran, M.C. Abt, L.K. Beura, P.J. Lucas, D. Artis, E.J. Wherry, K. Hogquist, et al. 2012. Antigen-independent differentiation and maintenance of effector-like resident memory T cells in tissues. *J. Immunol.* 188:4866–4875. http://dx.doi.org/10.4049/jimmunol.1200402

Christie, A., G.J. Davies-Wayne, T. Cordier-Lassalle, D.J. Blackley, A.S. Laney, D.E. Williams, S.A. Shinde, M. Badio, T. Lo, S.E. Mate, et al. Centers for Disease Control and Prevention. 2015. Possible sexual transmission of Ebola virus - Liberia, 2015. *MMWR Morb. Mortal. Wkly. Rep.* 64:479–481.

D'Ortenzio, E., S. Matheron, Y. Yazdanpanah, X. de Lamballerie, B. Hubert, G. Piorkowski, M. Maquart, D. Descamps, F. Damond, and I. Leparc-Goffart. 2016. Evidence of sexual transmission of Zika virus. *N. Engl. J. Med.* 374:2195–2198. http://dx.doi.org/10.1056/NEJMc1604449

Erlebacher, A. 2013. Mechanisms of T cell tolerance towards the allogeneic fetus. *Nat. Rev. Immunol.* 13:23–33. http://dx.doi.org/10.1038/nri3361

Fukao, T., and S. Koyasu. 2000. Expression of functional IL-2 receptors on mature splenic dendritic cells. *Eur. J. Immunol.* 30:1453–1457. http://dx.doi.org/10.1002/(SICI)1521-4141(200005)30:5<1453::AID-IMMU1453>3.0.CO;2-W

Fung-Leung, W.P., M.W. Schilham, A. Rahemtulla, T.M. Kündig, M. Vollenweider, J. Potter, W. van Ewijk, and T.W. Mak. 1991. CD8 is needed for development of cytotoxic T but not helper T cells. *Cell.* 65:443–449. http://dx.doi.org/10.1016/0092-8674(91)90462-8

Gill, N., P.M. Deacon, B. Lichty, K.L. Mossman, and A.A. Ashkar. 2006. Induction of innate immunity against herpes simplex virus type 2 infection via local delivery of Toll-like receptor ligands correlates with beta interferon production. *J. Virol.* 80:9943–9950. http://dx.doi.org/10.1128/JVI.01036-06

Grant, A., S.S. Ponia, S. Tripathi, V. Balasubramaniam, L. Miorin, M. Sourisseau, M.C. Schwarz, M.P. Sánchez-Seco, M.J. Evans, S.M. Best, and A. García-Sastre. 2016. Zika virus targets human STAT2 to inhibit type I interferon signaling. *Cell Host Microbe.* 19:882–890. http://dx.doi.org/10.1016/j.chom.2016.05.009

Granucci, F., D.M. Andrews, M.A. Degli-Esposti, and P. Ricciardi-Castagnoli. 2002. IL-2 mediates adjuvant effect of dendritic cells. *Trends Immunol.* 23:169–171. http://dx.doi.org/10.1016/S1471-4906(02)02187-7

Griffith, J.W., C.L. Sokol, and A.D. Luster. 2014. Chemokines and chemokine receptors: positioning cells for host defense and immunity. *Annu. Rev. Immunol.* 32:659–702. http://dx.doi.org/10.1146/annurev-immunol-032713-120145

Harrower, J., T. Kiedrzynski, S. Baker, A. Upton, F. Rahnama, J. Sherwood, Q.S. Huang, A. Todd, and D. Pulford. 2016. Sexual transmission of Zika virus and persistence in semen, New Zealand, 2016. *Emerg. Infect. Dis.* 22:1855–1857. http://dx.doi.org/10.3201/eid2210.160951

Herbst-Kralovetz, M.M., and R.B. Pyles. 2006. Quantification of poly(I:C)-mediated protection against genital herpes simplex virus type 2 infection. *J. Virol.* 80:9988–9997. http://dx.doi.org/10.1128/JVI.01099-06

Hsia, E., M.J. Johnston, R.J. Houlden, W.H. Chern, and H.E. Hofland. 2008. Effects of topically applied acitretin in reconstructed human epidermis and the rhino mouse. *J. Invest. Dermatol.* 128:125–130. http://dx.doi.org/10.1038/sj.jid.5700968

Iversen, M.B., L.S. Reinert, M.K. Thomsen, I. Bagdonaite, R. Nandakumar, N. Cheshenko, T. Prabakaran, S.Y. Vakhrushev, M. Krzyzowska, S.K. Kratholm, et al. 2016. An innate antiviral pathway acting before interferons at epithelial surfaces. *Nat. Immunol.* 17:150–158. http://dx.doi.org/10.1038/ni.3319

Iwasaki, A. 2007. Mucosal dendritic cells. *Annu. Rev. Immunol.* 25:381–418. http://dx.doi.org/10.1146/annurev.immunol.25.022106.141634

Iwasaki, A. 2010. Antiviral immune responses in the genital tract: clues for vaccines. *Nat. Rev. Immunol.* 10:699–711. http://dx.doi.org/10.1038/nri2836

Iwasaki, A., and R. Medzhitov. 2015. Control of adaptive immunity by the innate immune system. *Nat. Immunol.* 16:343–353. http://dx.doi.org/10.1038/ni.3123

Kumamoto, Y., and A. Iwasaki. 2012. Unique features of antiviral immune system of the vaginal mucosa. *Curr. Opin. Immunol.* 24:411–416. http://dx.doi.org/10.1016/j.coi.2012.05.006

Lazear, H.M., and M.S. Diamond. 2016. Zika virus: New clinical syndromes and its emergence in the Western hemisphere. *J. Virol.* 90:4864–4875. http://dx.doi.org/10.1128/JVI.00252-16

Lazear, H.M., J. Govero, A.M. Smith, D.J. Platt, E. Fernandez, J.J. Miner, and M.S. Diamond. 2016. A mouse model of Zika virus pathogenesis. *Cell Host Microbe.* 19:720–730. http://dx.doi.org/10.1016/j.chom.2016.03.010

Lessler, J., L.H. Chaisson, L.M. Kucirka, Q. Bi, K. Grantz, H. Salje, A.C. Carcelen, C.T. Ott, J.S. Sheffield, N.M. Ferguson, et al. 2016. Assessing the global threat from Zika virus. *Science.* 353:aaf8160. http://dx.doi.org/10.1126/science.aaf8160

Li, P., P. Kaiser, H.W. Lampiris, P. Kim, S.A. Yukl, D.V. Havlir, W.C. Greene, and J.K. Wong. 2016. Stimulating the RIG-I pathway to kill cells in the latent HIV reservoir following viral reactivation. *Nat. Med.* 22:807–811. http://dx.doi.org/10.1038/nm.4124

Madsen, L., N. Labrecque, J. Engberg, A. Dierich, A. Svejgaard, C. Benoist, D. Mathis, and L. Fugger. 1999. Mice lacking all conventional MHC class II genes. *Proc. Natl. Acad. Sci. USA.* 96:10338–10343. http://dx.doi.org/10.1073/pnas.96.18.10338

Mahlakõiv, T., P. Hernandez, K. Gronke, A. Diefenbach, and P. Staeheli. 2015. Leukocyte-derived IFN-α/β and epithelial IFN-λ constitute a compartmentalized mucosal defense system that restricts enteric virus infections. *PLoS Pathog.* 11:e1004782. http://dx.doi.org/10.1371/journal.ppat.1004782

Marks, E., M.A. Tam, and N.Y. Lycke. 2010. The female lower genital tract is a privileged compartment with IL-10 producing dendritic cells and poor Th1 immunity following *Chlamydia trachomatis* infection. *PLoS Pathog.* 6:e1001179. http://dx.doi.org/10.1371/journal.ppat.1001179

McCausland, M.M., and S. Crotty. 2008. Quantitative PCR technique for detecting lymphocytic choriomeningitis virus in vivo. *J. Virol. Methods.* 147:167–176. http://dx.doi.org/10.1016/j.jviromet.2007.08.025

Moldenhauer, L.M., K.R. Diener, D.M. Thring, M.P. Brown, J.D. Hayball, and S.A. Robertson. 2009. Cross-presentation of male seminal fluid antigens elicits T cell activation to initiate the female immune response to pregnancy. *J. Immunol.* 182:8080–8093. http://dx.doi.org/10.4049/jimmunol.0804018

Mombaerts, P., J. Iacomini, R.S. Johnson, K. Herrup, S. Tonegawa, and V.E. Papaioannou. 1992. RAG-1-deficient mice have no mature B and T lymphocytes. *Cell.* 68:869–877. http://dx.doi.org/10.1016/0092-8674(92)90030-G

Munoz-Suano, A., A.B. Hamilton, and A.G. Betz. 2011. Gimme shelter: the immune system during pregnancy. *Immunol. Rev.* 241:20–38. http://dx.doi.org/10.1111/j.1600-065X.2011.01002.x

Musso, D., C. Roche, E. Robin, T. Nhan, A. Teissier, and V.M. Cao-Lormeau. 2015. Potential sexual transmission of Zika virus. *Emerg. Infect. Dis.* 21:359–361. http://dx.doi.org/10.3201/eid2102.141363

Nurkkala, M., I. Nordström, E. Telemo, and K. Eriksson. 2007. MHC expression and chemokine production in the murine vagina following intra-vaginal administration of ligands to toll-like receptors 3, 7 and 9. *J. Reprod. Immunol.* 73:148–157. http://dx.doi.org/10.1016/j.jri.2006.09.001

Ochiel, D.O., M. Ghosh, J.V. Fahey, P.M. Guyre, and C.R. Wira. 2010. Human uterine epithelial cell secretions regulate dendritic cell differentiation and responses to TLR ligands. *J. Leukoc. Biol.* 88:435–444. http://dx.doi.org/10.1189/jlb.1009700

Oh, J.E., B.C. Kim, D.H. Chang, M. Kwon, S.Y. Lee, D. Kang, J.Y. Kim, I. Hwang, J.W. Yu, S. Nakae, and H.K. Lee. 2016. Dysbiosis-induced IL-33 contributes to impaired antiviral immunity in the genital mucosa. *Proc. Natl. Acad. Sci. USA.* 113:E762–E771. http://dx.doi.org/10.1073/pnas.1518589113

Olson, M.R., D.S. McDermott, and S.M. Varga. 2012. The initial draining lymph node primes the bulk of the CD8 T cell response and influences

memory T cell trafficking after a systemic viral infection. *PLoS Pathog.* 8:e1003054. http://dx.doi.org/10.1371/journal.ppat.1003054

Perez-Lopez, A., J. Behnsen, S.P. Nuccio, and M. Raffatellu. 2016. Mucosal immunity to pathogenic intestinal bacteria. *Nat. Rev. Immunol.* 16:135–148. http://dx.doi.org/10.1038/nri.2015.17

Pircher, H., D. Moskophidis, U. Rohrer, K. Bürki, H. Hengartner, and R.M. Zinkernagel. 1990. Viral escape by selection of cytotoxic T cell-resistant virus variants in vivo. *Nature.* 346:629–633. http://dx.doi.org/10.1038/346629a0

Rossi, S.L., R.B. Tesh, S.R. Azar, A.E. Muruato, K.A. Hanley, A.J. Auguste, R.M. Langsjoen, S. Paessler, N. Vasilakis, and S.C. Weaver. 2016. Characterization of a novel murine model to study Zika virus. *Am. J. Trop. Med. Hyg.* 94:1362–1369. http://dx.doi.org/10.4269/ajtmh.16-0111

Sato, M., H. Suemori, N. Hata, M. Asagiri, K. Ogasawara, K. Nakao, T. Nakaya, M. Katsuki, S. Noguchi, N. Tanaka, and T. Taniguchi. 2000. Distinct and essential roles of transcription factors IRF-3 and IRF-7 in response to viruses for *IFN-α/β* gene induction. *Immunity.* 13:539–548. http://dx.doi.org/10.1016/S1074-7613(00)00053-4

Schenkel, J.M., K.A. Fraser, V. Vezys, and D. Masopust. 2013. Sensing and alarm function of resident memory $CD8^+$ T cells. *Nat. Immunol.* 14:509–513. http://dx.doi.org/10.1038/ni.2568

Stary, G., A. Olive, A.F. Radovic-Moreno, D. Gondek, D. Alvarez, P.A. Basto, M. Perro, V.D. Vrbanac, A.M. Tager, J. Shi, et al. 2015. A mucosal vaccine against *Chlamydia trachomatis* generates two waves of protective memory T cells. *Science.* 348:aaa8205. http://dx.doi.org/10.1126/science.aaa8205

Suvas, P.K., H.M. Dech, F. Sambira, J. Zeng, and T.M. Onami. 2007. Systemic and mucosal infection program protective memory CD8 T cells in the vaginal mucosa. *J. Immunol.* 179:8122–8127. http://dx.doi.org/10.4049/jimmunol.179.12.8122

Takeuchi, O., and S. Akira. 2010. Pattern recognition receptors and inflammation. *Cell.* 140:805–820. http://dx.doi.org/10.1016/j.cell.2010.01.022

Trinchieri, G. 2010. Type I interferon: friend or foe? *J. Exp. Med.* 207:2053–2063. http://dx.doi.org/10.1084/jem.20101664

Turmel, J.M., P. Abgueguen, B. Hubert, Y.M. Vandamme, M. Maquart, H. Le Guillou-Guillemette, and I. Leparc-Goffart. 2016. Late sexual transmission of Zika virus related to persistence in the semen. *Lancet.* 387:2501. http://dx.doi.org/10.1016/S0140-6736(16)30775-9

Warning, J.C., S.A. McCracken, and J.M. Morris. 2011. A balancing act: mechanisms by which the fetus avoids rejection by the maternal immune system. *Reproduction.* 141:715–724. http://dx.doi.org/10.1530/REP-10-0360

Wira, C.R., M. Rodriguez-Garcia, and M.V. Patel. 2015. The role of sex hormones in immune protection of the female reproductive tract. *Nat. Rev. Immunol.* 15:217–230. http://dx.doi.org/10.1038/nri3819

Wuest, S.C., J.H. Edwan, J.F. Martin, S. Han, J.S. Perry, C.M. Cartagena, E. Matsuura, D. Maric, T.A. Waldmann, and B. Bielekova. 2011. A role for interleukin-2 trans-presentation in dendritic cell-mediated T cell activation in humans, as revealed by daclizumab therapy. *Nat. Med.* 17:604–609. http://dx.doi.org/10.1038/nm.2365

Yiu, Z.Z., R.B. Warren, U. Mrowietz, and C.E. Griffiths. 2015. Safety of conventional systemic therapies for psoriasis on reproductive potential and outcomes. *J. Dermatolog. Treat.* 26:329–334. http://dx.doi.org/10.3109/09546634.2014.991673

Yockey, L.J., L. Varela, T. Rakib, W. Khoury-Hanold, S.L. Fink, B. Stutz, K. Szigeti-Buck, A. Van den Pol, B.D. Lindenbach, T.L. Horvath, and A. Iwasaki. 2016. Vaginal exposure to Zika virus during pregnancy leads to fetal brain infection. *Cell.* 166:1247–1256.e4. http://dx.doi.org/10.1016/j.cell.2016.08.004

Zhao, X., E. Deak, K. Soderberg, M. Linehan, D. Spezzano, J. Zhu, D.M. Knipe, and A. Iwasaki. 2003. Vaginal submucosal dendritic cells, but not Langerhans cells, induce protective Th1 responses to herpes simplex virus-2. *J. Exp. Med.* 197:153–162. http://dx.doi.org/10.1084/jem.20021109

Zhou, X., S. Ramachandran, M. Mann, and D.L. Popkin. 2012. Role of lymphocytic choriomeningitis virus (LCMV) in understanding viral immunology: past, present and future. *Viruses.* 4:2650–2669. http://dx.doi.org/10.3390/v4112650